

## Semileptonic $B$ decays to excited charmed mesons

Adam K. Leibovich, Zoltan Ligeti, Iain W. Stewart, Mark B. Wise  
*California Institute of Technology, Pasadena, CA 91125*

### Abstract

Exclusive semileptonic  $B$  decays into excited charmed mesons are investigated at order  $\Lambda_{\text{QCD}}/m_Q$  in the heavy quark effective theory. Differential decay rates for each helicity state of the four lightest excited  $D$  mesons ( $D_1$ ,  $D_2^*$ ,  $D_0^*$ , and  $D_1^*$ ) are examined. At zero recoil,  $\Lambda_{\text{QCD}}/m_Q$  corrections to the matrix elements of the weak currents can be written in terms of the leading Isgur-Wise functions for the corresponding transition and meson mass splittings. A model independent prediction is found for the slope parameter of the decay rate into helicity zero  $D_1$  at zero recoil. The differential decay rates are predicted, including  $\Lambda_{\text{QCD}}/m_Q$  corrections with some model dependence away from zero recoil and including order  $\alpha_s$  corrections. Ratios of various exclusive branching ratios are computed. Matrix elements of the weak currents between  $B$  mesons and other excited charmed mesons are discussed at zero recoil to order  $\Lambda_{\text{QCD}}/m_Q$ . These amplitudes vanish at leading order, and can be written at order  $\Lambda_{\text{QCD}}/m_Q$  in terms of local matrix elements. Applications to  $B$  decay sum rules and factorization are presented.

## I. INTRODUCTION

Heavy quark symmetry [1] implies that in the  $m_Q \rightarrow \infty$  limit matrix elements of the weak currents between a  $B$  meson and an excited charmed meson vanish at zero recoil (where in the rest frame of the  $B$  the final state charmed meson is also at rest). However, in some cases at order  $\Lambda_{\text{QCD}}/m_Q$  these matrix elements are not zero [2]. Since most of the phase space for semileptonic  $B$  decay to excited charmed mesons is near zero recoil,  $\Lambda_{\text{QCD}}/m_Q$  corrections can be very important. This paper is concerned with rates for  $B$  semileptonic decay to excited charmed mesons, including the effects of  $\Lambda_{\text{QCD}}/m_Q$  corrections.

The use of heavy quark symmetry resulted in a dramatic improvement in our understanding of the spectroscopy and weak decays of hadrons containing a single heavy quark,  $Q$ . In the limit where the heavy quark mass goes to infinity,  $m_Q \rightarrow \infty$ , such hadrons are classified not only by their total spin  $J$ , but also by the spin of their light degrees of freedom (i.e., light quarks and gluons),  $s_\ell$  [3]. In this limit hadrons containing a single heavy quark come in degenerate doublets with total spin,  $J_\pm = s_\ell \pm \frac{1}{2}$ , coming from combining the spin of the light degrees of freedom with the spin of the heavy quark,  $s_Q = \frac{1}{2}$ . (An exception occurs for baryons with  $s_\ell = 0$ , where there is only a single state with  $J = \frac{1}{2}$ .) The ground state mesons with  $Q\bar{q}$  flavor quantum numbers contain light degrees of freedom with spin-parity  $s_\ell^{\pi_\ell} = \frac{1}{2}^-$ , giving a doublet containing a spin zero and spin one meson. For  $Q = c$  these mesons are the  $D$  and  $D^*$ , while  $Q = b$  gives the  $B$  and  $B^*$  mesons.

Excited charmed mesons with  $s_\ell^{\pi_\ell} = \frac{3}{2}^+$  have been observed. These are the  $D_1$  and  $D_2^*$  mesons with spin one and two, respectively. (There is also evidence for the analogous  $Q = b$  heavy meson doublet.) For  $q = u, d$ , the  $D_1$  and  $D_2^*$  mesons have been observed to decay to  $D^{(*)}\pi$  and are narrow with widths around 20 MeV. (The  $D_{s1}$  and  $D_{s2}^*$  strange mesons decay to  $D^{(*)}K$ .) In the nonrelativistic constituent quark model these states correspond to  $L = 1$  orbital excitations. Combining the unit of orbital angular momentum with the spin of the light antiquark leads to states with  $s_\ell^{\pi_\ell} = \frac{1}{2}^+$  and  $\frac{3}{2}^+$ . The  $\frac{1}{2}^+$  doublet,  $(D_0^*, D_1^*)$ , has not been observed. Presumably this is because these states are much broader than those with  $s_\ell^{\pi_\ell} = \frac{3}{2}^+$ . A vast discrepancy in widths is expected since the members of the  $\frac{1}{2}^+$  doublet of charmed mesons decay to  $D^{(*)}\pi$  in an  $S$ -wave while the members of the  $\frac{3}{2}^+$  doublet of charmed mesons decay to  $D^{(*)}\pi$  in a  $D$ -wave. (An  $S$ -wave  $D_1 \rightarrow D^*\pi$  amplitude is allowed by total angular momentum conservation, but forbidden in the  $m_Q \rightarrow \infty$  limit by heavy quark spin symmetry [3].)

The heavy quark effective theory (HQET) is the limit of QCD where the heavy quark mass goes to infinity with its four velocity,  $v$ , fixed. The heavy quark field in QCD,  $Q$ , is related to its counterpart in HQET,  $h_v^{(Q)}$ , by

$$Q(x) = e^{-im_Q v \cdot x} \left[ 1 + \frac{i\not{D}}{2m_Q} + \dots \right] h_v^{(Q)}, \quad (1.1)$$

where  $\not{D}h_v^{(Q)} = h_v^{(Q)}$  and the ellipses denote terms suppressed by further powers of  $\Lambda_{\text{QCD}}/m_Q$ . Putting Eq. (1.1) into the part of the QCD Lagrangian involving the heavy quark field,  $\mathcal{L} = \bar{Q}(i\not{D} - m_Q)Q$ , gives

$$\mathcal{L} = \mathcal{L}_{\text{HQET}} + \delta\mathcal{L} + \dots \quad (1.2)$$

The HQET Lagrangian [4]

$$\mathcal{L}_{\text{HQET}} = \bar{h}_v^{(Q)} i v \cdot D h_v^{(Q)} \quad (1.3)$$

is independent of the mass of the heavy quark and its spin, and so for  $N_Q$  heavy quarks with the same four velocity  $v$  there is a  $U(2N_Q)$  spin-flavor symmetry. This symmetry is broken by the order  $\Lambda_{\text{QCD}}/m_Q$  terms [5] in  $\delta\mathcal{L}$ ,

$$\delta\mathcal{L} = \frac{1}{2m_Q} [O_{\text{kin},v}^{(Q)} + O_{\text{mag},v}^{(Q)}], \quad (1.4)$$

where

$$O_{\text{kin},v}^{(Q)} = \bar{h}_v^{(Q)} (iD)^2 h_v^{(Q)}, \quad O_{\text{mag},v}^{(Q)} = \bar{h}_v^{(Q)} \frac{g_s}{2} \sigma_{\alpha\beta} G^{\alpha\beta} h_v^{(Q)}. \quad (1.5)$$

The first term in Eq. (1.4) is the heavy quark kinetic energy. It breaks the flavor symmetry but leaves the spin symmetry intact. The second is the chromomagnetic term, which breaks both the spin and flavor symmetries. (In the rest frame, it is of the form  $\vec{\mu}_Q \cdot \vec{B}_{\text{color}}$ , where  $\vec{\mu}_Q$  is the heavy quark color magnetic moment.)

The hadron masses give important information on some HQET matrix elements. The mass formula for a spin symmetry doublet of hadrons  $H_{\pm}$  with total spin  $J_{\pm} = s_{\ell} \pm \frac{1}{2}$  is

$$m_{H_{\pm}} = m_Q + \bar{\Lambda}^H - \frac{\lambda_1^H}{2m_Q} \pm \frac{n_{\mp} \lambda_2^H}{2m_Q} + \dots, \quad (1.6)$$

where the ellipsis denote terms suppressed by more powers of  $\Lambda_{\text{QCD}}/m_Q$  and  $n_{\pm} = 2J_{\pm} + 1$  is the number of spin states in the hadron  $H_{\pm}$ . The parameter  $\bar{\Lambda}$  is the energy of the light degrees of freedom in the  $m_Q \rightarrow \infty$  limit,  $\lambda_1$  determines the heavy quark kinetic energy<sup>1</sup>

$$\lambda_1^H = \frac{1}{2v^0 m_{H_{\pm}}} \langle H_{\pm}(v) | \bar{h}_v^{(Q)} (iD)^2 h_v^{(Q)} | H_{\pm}(v) \rangle, \quad (1.7)$$

and  $\lambda_2$  determines the chromomagnetic energy

$$\lambda_2^H = \frac{\mp 1}{2v^0 m_{H_{\pm}} n_{\mp}} \langle H_{\pm}(v) | \bar{h}_v^{(Q)} \frac{g_s}{2} \sigma_{\alpha\beta} G^{\alpha\beta} h_v^{(Q)} | H_{\pm}(v) \rangle. \quad (1.8)$$

$\bar{\Lambda}$  and  $\lambda_1$  are independent of the heavy quark mass, while  $\lambda_2$  has a weak logarithmic dependence on  $m_Q$ . Of course they depend on the particular spin symmetry doublet to which  $H_{\pm}$  belong. In this paper, we consider heavy mesons in the ground state  $s_{\ell}^{\pi\ell} = \frac{1}{2}^-$  doublet and the excited  $s_{\ell}^{\pi\ell} = \frac{3}{2}^+$  and  $\frac{1}{2}^+$  doublets. We reserve the notation  $\bar{\Lambda}$ ,  $\lambda_1$ ,  $\lambda_2$  for the ground state multiplet and use  $\bar{\Lambda}'$ ,  $\lambda_1'$ ,  $\lambda_2'$  and  $\bar{\Lambda}^*$ ,  $\lambda_1^*$ ,  $\lambda_2^*$  for the excited  $s_{\ell}^{\pi\ell} = \frac{3}{2}^+$  and  $\frac{1}{2}^+$  doublets, respectively.

---

<sup>1</sup>Hadron states labeled by their four-velocity,  $v = p_H/m_H$ , satisfy the standard covariant normalization  $\langle H(p'_H) | H(p_H) \rangle = (2\pi)^3 2E_H \delta^3(\vec{p}'_H - \vec{p}_H)$ .

$s_l^{\pi_l}$	Particles	$J^P$	$\bar{m}$ (GeV)
$\frac{1}{2}^-$	$D, D^*$	$0^-, 1^-$	1.971
$\frac{1}{2}^+$	$D_0^*, D_1^*$	$0^+, 1^+$	$\sim 2.40$
$\frac{3}{2}^+$	$D_1, D_2^*$	$1^+, 2^+$	2.445

TABLE I. Charmed meson spin multiplets ( $q = u, d$ ).

The average mass  $\bar{m}_H$ , weighted by the number of helicity states

$$\bar{m}_H = \frac{n_- m_{H_-} + n_+ m_{H_+}}{n_+ + n_-}, \quad (1.9)$$

is independent of  $\lambda_2$ . The spin average masses for the lowest lying charmed mesons is given in Table I. Identifying the  $B^{(*)}\pi$  resonances observed at LEP with the bottom  $s_\ell^{\pi_\ell} = \frac{3}{2}^+$  meson doublet we can use their average mass,  $\bar{m}'_B = 5.73$  GeV [6], to determine the differences  $\bar{\Lambda}' - \bar{\Lambda}$  and  $\lambda'_1 - \lambda_1$ :

$$\begin{aligned} \bar{\Lambda}' - \bar{\Lambda} &= \frac{m_b (\bar{m}'_B - \bar{m}_B) - m_c (\bar{m}'_D - \bar{m}_D)}{m_b - m_c} \simeq 0.39 \text{ GeV}, \\ \lambda'_1 - \lambda_1 &= \frac{2m_c m_b [(\bar{m}'_B - \bar{m}_B) - (\bar{m}'_D - \bar{m}_D)]}{m_b - m_c} \simeq -0.23 \text{ GeV}^2. \end{aligned} \quad (1.10)$$

The numerical values in Eq. (1.10) follow from the choices  $m_b = 4.8$  GeV and  $m_c = 1.4$  GeV. To the order we are working,  $m_b$  and  $m_c$  in Eq. (1.10) can be replaced by  $\bar{m}_B$  and  $\bar{m}_D$ . This changes the value of  $\bar{\Lambda}' - \bar{\Lambda}$  only slightly, but has a significant impact on the value of  $\lambda'_1 - \lambda_1$ . The value of  $\bar{\Lambda}' - \bar{\Lambda}$  given in Eq. (1.10) has considerable uncertainty because the experimental error on  $\bar{m}'_B$  is large, and because it is not clear that the peak of the  $B^{(*)}\pi$  mass distribution corresponds to the narrow  $\frac{3}{2}^+$  doublet.<sup>2</sup>

At the present time,  $\bar{\Lambda}$  and  $\lambda_1$  are not well determined. A fit to the electron energy spectrum in semileptonic  $B$  decay gives [7]  $\bar{\Lambda} \simeq 0.4$  GeV and  $\lambda_1 \simeq -0.2$  GeV<sup>2</sup>, but the uncertainties are quite large [8]. (A linear combination of  $\bar{\Lambda}$  and  $\lambda_1$  is better determined than the individual values.)

The measured  $D^* - D$  mass difference (142 MeV) and the measured  $D_2^* - D_1$  mass difference (37 MeV) fix  $\lambda_2 = 0.10$  GeV<sup>2</sup> and  $\lambda'_2 = 0.013$  GeV<sup>2</sup>. Note that the matrix element of the

<sup>2</sup>The  $B_{s1}$  and  $B_{s2}^*$  masses could also be used to determine  $\bar{\Lambda}' - \bar{\Lambda}$  from the relation

$$\bar{\Lambda}' - \bar{\Lambda} = \bar{\Lambda}'_s - \bar{\Lambda} + (\bar{m}'_D - \bar{m}'_{D_s}) + \mathcal{O}(\Lambda_{\text{QCD}} m_s/m_c),$$

with the analog of Eq. (1.10) used to fix  $\bar{\Lambda}'_s - \bar{\Lambda}$ , and  $\bar{m}'_D - \bar{m}'_{D_s} = -114$  MeV. The  $B_s^*$  has not been observed, but its mass can be determined from  $(m_{B_s^*} - m_{B_s}) - (m_{B^*} - m_B) = (m_c/m_b) [(m_{D_s^*} - m_{D_s}) - (m_{D^*} - m_D)]$ . However, because of uncertainties in the  $B_{s1}$  and  $B_{s2}^*$  masses and the unknown order ( $\Lambda_{\text{QCD}} m_s/m_c$ ) term, this relation does not give a more reliable determination of  $\bar{\Lambda}' - \bar{\Lambda}$  than Eq. (1.10).

chromomagnetic operator is substantially smaller in the excited  $s_\ell^{\pi\ell} = \frac{3}{2}^+$  multiplet than in the ground state multiplet. This is consistent with expectations based on the nonrelativistic constituent quark model. In this phenomenological model, the splitting between members of a  $Q\bar{q}$  meson spin symmetry doublet arises mostly from matrix elements of the operator  $\vec{s}_Q \cdot \vec{s}_{\bar{q}} \delta^3(\vec{r})$ , and these vanish for  $Q\bar{q}$  mesons with orbital angular momentum.

Semileptonic  $B$  meson decays have been studied extensively. The semileptonic decays  $B \rightarrow D e \bar{\nu}_e$  and  $B \rightarrow D^* e \bar{\nu}_e$  have branching ratios of  $(1.8 \pm 0.4)\%$  and  $(4.6 \pm 0.3)\%$ , respectively [9], and comprise about 60% of the semileptonic decays. The differential decay rates for these decays are determined by matrix elements of the weak  $b \rightarrow c$  axial-vector and vector currents between the  $B$  meson and the recoiling  $D^{(*)}$  meson. These matrix elements are usually parameterized by a set of Lorentz scalar form factors and the differential decay rate is expressed in terms of these form factors. For comparison with the predictions of HQET, it is convenient to write the form factors as functions of the dot-product,  $w = v \cdot v'$ , of the four-velocity of the  $B$  meson,  $v$ , and that of the recoiling  $D^{(*)}$  meson,  $v'$ . In the  $m_Q \rightarrow \infty$  limit, heavy quark spin symmetry implies that the six form factors that parameterize the  $B \rightarrow D$  and  $B \rightarrow D^*$  matrix elements of the  $b \rightarrow c$  axial-vector and vector currents can be written in terms of a single function of  $w$  [1]. Furthermore, heavy quark flavor symmetry implies that this function is normalized to unity at zero recoil,  $w = 1$ , where the  $D^{(*)}$  is at rest in the rest frame of the  $B$  [10,11,1]. The functions of  $w$  that occur in predictions for weak decay form factors based on HQET are usually called Isgur-Wise functions. There are perturbative  $\alpha_s(m_Q)$  and nonperturbative  $\Lambda_{\text{QCD}}/m_Q$  corrections to the predictions of the  $m_Q \rightarrow \infty$  limit for the  $B \rightarrow D^{(*)} e \bar{\nu}_e$  semileptonic decay form factors. The perturbative QCD corrections do not cause any loss of predictive power. They involve the same Isgur-Wise function that occurs in the  $m_Q \rightarrow \infty$  limit. At order  $\Lambda_{\text{QCD}}/m_Q$  several new Isgur-Wise functions occur; however, at zero recoil, there are no  $\Lambda_{\text{QCD}}/m_Q$  corrections [12]. Expectations for the  $B \rightarrow D^{(*)} e \bar{\nu}_e$  differential decay rate based on HQET are in agreement with experiment [13].

Recently, semileptonic  $B$  decay to an excited heavy meson has been observed [14–16]. With some assumptions, CLEO [16] and ALEPH [15] find respectively the branching ratios  $\mathcal{B}(B \rightarrow D_1 e \bar{\nu}_e) = (0.49 \pm 0.14)\%$  and  $\mathcal{B}(B \rightarrow D_1^* e \bar{\nu}_e) = (0.74 \pm 0.16)\%$ , as well as the limits  $\mathcal{B}(B \rightarrow D_2^* e \bar{\nu}_e) < 1\%$  and  $\mathcal{B}(B \rightarrow D_2^* e \bar{\nu}_e) < 0.2\%$ . In the future it should be possible to get detailed experimental information on the  $B \rightarrow D_1 e \bar{\nu}_e$  and  $B \rightarrow D_2^* e \bar{\nu}_e$  differential decay rates.

In this paper we study the predictions of HQET for  $B$  semileptonic decay to excited charmed mesons. This paper elaborates on the work in Ref. [2] and contains some new results. In the infinite mass limit the matrix elements of the weak axial-vector and vector current between the  $B$  meson and any excited charmed meson vanish at zero recoil by heavy quark symmetry. Corrections to the infinite mass limit of order  $\Lambda_{\text{QCD}}/m_Q$  and order  $\alpha_s(m_Q)$  are discussed. The corrections of order  $\Lambda_{\text{QCD}}/m_Q$  are very important, particularly near zero recoil.

Section II discusses the differential decay rate  $d^2\Gamma/dw d\cos\theta$  for  $B \rightarrow (D_1, D_2^*) e \bar{\nu}_e$ , where  $\theta$  is the angle between the the charged lepton and the charmed meson in the rest frame of the virtual  $W$  boson. Corrections of order  $\Lambda_{\text{QCD}}/m_Q$  are included. At order  $\Lambda_{\text{QCD}}/m_Q$  the  $B \rightarrow D_1$  zero recoil matrix element does not vanish and is expressible in terms of the

leading  $m_Q \rightarrow \infty$  Isgur-Wise function,  $\tau$ , and  $\bar{\Lambda}' - \bar{\Lambda}$  (which is known in terms of hadron mass splittings from Eq. (1.10)). Away from zero recoil new Isgur-Wise functions occur, which are unknown. These introduce a significant uncertainty. The  $\Lambda_{\text{QCD}}/m_Q$  corrections enhance considerably the  $B$  semileptonic decay rate to the  $D_1$  state, and for zero helicity the slope of  $d\Gamma(B \rightarrow D_1 e \bar{\nu}_e)/dw$  at  $w = 1$  is predicted. These corrections also reduce the ratio  $R = \mathcal{B}(B \rightarrow D_2^* e \bar{\nu}_e)/\mathcal{B}(B \rightarrow D_1 e \bar{\nu}_e)$  compared to its value in the  $m_Q \rightarrow \infty$  limit. The value of  $\tau$  at zero recoil is not fixed by heavy quark symmetry, and must be determined from experiment. The measured  $B \rightarrow D_1 e \bar{\nu}_e$  branching ratio is used to determine (with some model dependent assumptions)  $|\tau(1)| = 0.71$ . The effects of perturbative QCD corrections are also discussed, with further details given in Appendix A.

It is interesting to understand the composition of the inclusive  $B$  semileptonic decay rate in terms of exclusive final states. In Section III, the HQET predictions for the differential decay rates for  $B \rightarrow D_0^* e \bar{\nu}_e$  and  $B \rightarrow D_1^* e \bar{\nu}_e$  are investigated. The situation for the excited  $s_\ell^{\pi_\ell} = \frac{1}{2}^+$  multiplet is similar to the  $s_\ell^{\pi_\ell} = \frac{3}{2}^+$  multiplet discussed in Section II. Using a quark model relation between the leading  $m_Q \rightarrow \infty$  Isgur-Wise functions for  $B$  decays to the  $s_\ell^{\pi_\ell} = \frac{3}{2}^+$  and  $s_\ell^{\pi_\ell} = \frac{1}{2}^+$  charmed mesons (and some other model dependent assumptions), the rates for  $B \rightarrow D_0^* e \bar{\nu}_e$  and  $B \rightarrow D_1^* e \bar{\nu}_e$  are predicted.

Section IV discusses the contribution of other excited charmed mesons to the matrix elements of the vector and axial-vector current at zero recoil. Only excited charmed hadrons with  $s_\ell^{\pi_\ell} = \frac{1}{2}^-$ ,  $\frac{3}{2}^-$  and  $\frac{1}{2}^+$ ,  $\frac{3}{2}^+$  can contribute. The  $\frac{3}{2}^+$  and  $\frac{1}{2}^+$  doublets are discussed in Sections II and III. This section deals with the  $\frac{1}{2}^-$  and  $\frac{3}{2}^-$  cases, where the  $\Lambda_{\text{QCD}}/m_Q$  corrections to the states from  $\delta\mathcal{L}$  give rise to non-vanishing zero recoil matrix elements.

Section V examines other applications of our results. Using factorization, predictions are made for nonleptonic  $B$  decay widths to  $D_2^* \pi$ ,  $D_1 \pi$  and to  $D_1^* \pi$ ,  $D_0^* \pi$ . The importance of our results for  $B$  decay sum rules is discussed. Including the excited states dramatically strengthens the Bjorken lower bound on the slope of the  $B \rightarrow D^{(*)} e \bar{\nu}_e$  Isgur-Wise function.

Concluding remarks and a summary of our most significant predictions are given in Section VI.

## II. $B \rightarrow D_1 e \bar{\nu}_e$ AND $B \rightarrow D_2^* e \bar{\nu}_e$ DECAYS

The matrix elements of the vector and axial-vector currents ( $V^\mu = \bar{c} \gamma^\mu b$  and  $A^\mu = \bar{c} \gamma^\mu \gamma_5 b$ ) between  $B$  mesons and  $D_1$  or  $D_2^*$  mesons can be parameterized as

$$\begin{aligned}
\frac{\langle D_1(v', \epsilon) | V^\mu | B(v) \rangle}{\sqrt{m_{D_1} m_B}} &= f_{V_1} \epsilon^{*\mu} + (f_{V_2} v^\mu + f_{V_3} v'^\mu) (\epsilon^* \cdot v), \\
\frac{\langle D_1(v', \epsilon) | A^\mu | B(v) \rangle}{\sqrt{m_{D_1} m_B}} &= i f_A \epsilon^{\mu\alpha\beta\gamma} \epsilon_\alpha^* v_\beta v'_\gamma, \\
\frac{\langle D_2^*(v', \epsilon) | A^\mu | B(v) \rangle}{\sqrt{m_{D_2^*} m_B}} &= k_{A_1} \epsilon^{*\mu\alpha} v_\alpha + (k_{A_2} v^\mu + k_{A_3} v'^\mu) \epsilon_{\alpha\beta}^* v^\alpha v'^\beta, \\
\frac{\langle D_2^*(v', \epsilon) | V^\mu | B(v) \rangle}{\sqrt{m_{D_2^*} m_B}} &= i k_V \epsilon^{\mu\alpha\beta\gamma} \epsilon_{\alpha\sigma}^* v^\sigma v_\beta v'_\gamma,
\end{aligned} \tag{2.1}$$

where the form factors  $f_i$  and  $k_i$  are dimensionless functions of  $w$ . At zero recoil ( $v = v'$ ) only the  $f_{V_1}$  form factor can contribute, since  $v'$  dotted into the polarization ( $\epsilon^{*\mu}$  or  $\epsilon^{*\mu\alpha}$ ) vanishes.

The differential decay rates can be written in terms of the form factors in Eq. (2.1). It is useful to separate the contributions to the different helicities of the  $D_1$  and  $D_2^*$  mesons, since the  $\Lambda_{\text{QCD}}/m_Q$  corrections effect these differently, and the decay rates into different helicity states will probably be measurable. We define  $\theta$  as the angle between the charged lepton and the charmed meson in the rest frame of the virtual  $W$  boson, i.e., in the center of momentum frame of the lepton pair. The different helicity amplitudes yield different distributions in  $\theta$ . In terms of  $w = v \cdot v'$  and  $\theta$ , the double differential decay rates are

$$\begin{aligned} \frac{d^2\Gamma_{D_1}}{dw d\cos\theta} &= 3\Gamma_0 r_1^3 \sqrt{w^2 - 1} \left\{ \sin^2\theta \left[ (w - r_1)f_{V_1} + (w^2 - 1)(f_{V_3} + r_1 f_{V_2}) \right]^2 \right. \\ &\quad \left. + (1 - 2r_1 w + r_1^2) \left[ (1 + \cos^2\theta) [f_{V_1}^2 + (w^2 - 1)f_A^2] - 4\cos\theta \sqrt{w^2 - 1} f_{V_1} f_A \right] \right\}, \\ \frac{d^2\Gamma_{D_2^*}}{dw d\cos\theta} &= \frac{3}{2}\Gamma_0 r_2^3 (w^2 - 1)^{3/2} \left\{ \frac{4}{3} \sin^2\theta \left[ (w - r_2)k_{A_1} + (w^2 - 1)(k_{A_3} + r_2 k_{A_2}) \right]^2 \right. \\ &\quad \left. + (1 - 2r_2 w + r_2^2) \left[ (1 + \cos^2\theta) [k_{A_1}^2 + (w^2 - 1)k_V^2] - 4\cos\theta \sqrt{w^2 - 1} k_{A_1} k_V \right] \right\}, \end{aligned} \quad (2.2)$$

where  $\Gamma_0 = G_F^2 |V_{cb}|^2 m_B^5 / (192\pi^3)$ ,  $r_1 = m_{D_1}/m_B$ ,  $r_2 = m_{D_2^*}/m_B$ . The semileptonic  $B$  decay rate into any  $J \neq 1$  state involves an extra factor of  $w^2 - 1$ . The  $\sin^2\theta$  term is the helicity zero rate, while the  $1 + \cos^2\theta$  and  $\cos\theta$  terms determine the helicity  $\lambda = \pm 1$  rates. Since the weak current is  $V - A$  in the standard model,  $B$  mesons can only decay into the helicity  $|\lambda| = 0, 1$  components of any excited charmed mesons. The decay rate for  $|\lambda| = 1$  vanishes at maximal recoil,  $w_{\text{max}} = (1 + r^2)/(2r)$ , as implied by the  $1 - 2rw + r^2$  factors above ( $r = r_1$  or  $r_2$ ). From Eq. (2.2) it is straightforward to obtain the double differential rate  $d^2\Gamma/dw dy$  using the relation

$$y = 1 - rw - r\sqrt{w^2 - 1} \cos\theta, \quad (2.3)$$

where  $y = 2E_e/m_B$  is the rescaled lepton energy.

The form factors  $f_i$  and  $k_i$  can be parameterized by a set of Isgur-Wise functions at each order in  $\Lambda_{\text{QCD}}/m_Q$ . It is simplest to calculate the matrix elements in Eq. (2.1) using the trace formalism [17,18]. The fields  $P_v$  and  $P_v^{*\mu}$  that destroy members of the  $s_l^{\pi^i} = \frac{1}{2}^-$  doublet with four-velocity  $v$  are in the  $4 \times 4$  matrix

$$H_v = \frac{1 + \not{v}}{2} \left[ P_v^{*\mu} \gamma_\mu - P_v \gamma_5 \right]. \quad (2.4)$$

while for  $s_l^{\pi^i} = \frac{3}{2}^+$  the fields  $P_v^\nu$  and  $P_v^{*\mu\nu}$  are in

$$F_v^\mu = \frac{1 + \not{v}}{2} \left\{ P_v^{*\mu\nu} \gamma_\nu - \sqrt{\frac{3}{2}} P_v^\nu \gamma_5 \left[ g_\nu^\mu - \frac{1}{3} \gamma_\nu (\gamma^\mu - v^\mu) \right] \right\}. \quad (2.5)$$

The matrices  $H$  and  $F$  satisfy the properties  $\not{v}H_v = H_v = -H_v\not{v}$ ,  $\not{v}F_v^\mu = F_v^\mu = -F_v^\mu\not{v}$ , and  $F_v^\mu \gamma_\mu = F_v^\mu v_\mu = 0$ .

To leading order in  $\Lambda_{\text{QCD}}/m_Q$  and  $\alpha_s$ , matrix elements of the  $b \rightarrow c$  flavor changing current between the states destroyed by the fields in  $H_v$  and  $F_{v'}^\sigma$  are

$$\bar{c} \Gamma b = \bar{h}_{v'}^{(c)} \Gamma h_v^{(b)} = \tau(w) \text{Tr} \left\{ v_\sigma \bar{F}_{v'}^\sigma \Gamma H_v \right\}. \quad (2.6)$$

Here  $\tau(w)$  is a dimensionless function, and  $h_v^{(Q)}$  is the heavy quark field in the effective theory ( $\tau$  is  $\sqrt{3}$  times the function  $\tau_{3/2}$  of Ref. [19]). This matrix element vanishes at zero recoil for any Dirac structure  $\Gamma$  and for any value of  $\tau(1)$ , since the  $B$  meson and the  $(D_1, D_2^*)$  mesons are in different heavy quark spin symmetry multiplets, and the current at zero recoil is related to the conserved charges of heavy quark spin-flavor symmetry. Eq. (2.6) leads to the  $m_Q \rightarrow \infty$  predictions for the form factors  $f_i$  and  $k_i$  given in Ref. [19].

At order  $\Lambda_{\text{QCD}}/m_Q$ , there are corrections originating from the matching of the  $b \rightarrow c$  flavor changing current onto the effective theory, and from order  $\Lambda_{\text{QCD}}/m_Q$  corrections to the effective Lagrangian. The current corrections modify the first equality in Eq. (2.6) to

$$\bar{c} \Gamma b = \bar{h}_{v'}^{(c)} \left( \Gamma - \frac{i}{2m_c} \overleftarrow{D} \Gamma + \frac{i}{2m_b} \Gamma \overrightarrow{D} \right) h_v^{(b)}. \quad (2.7)$$

For matrix elements between the states destroyed by the fields in  $F_{v'}^\sigma$  and  $H_v$ , the new order  $\Lambda_{\text{QCD}}/m_Q$  operators in Eq. (2.7) are

$$\begin{aligned} \bar{h}_{v'}^{(c)} i \overleftarrow{D}_\lambda \Gamma h_v^{(b)} &= \text{Tr} \left\{ \mathcal{S}_{\sigma\lambda}^{(c)} \bar{F}_{v'}^\sigma \Gamma H_v \right\}, \\ \bar{h}_{v'}^{(c)} \Gamma i \overrightarrow{D}_\lambda h_v^{(b)} &= \text{Tr} \left\{ \mathcal{S}_{\sigma\lambda}^{(b)} \bar{F}_{v'}^\sigma \Gamma H_v \right\}. \end{aligned} \quad (2.8)$$

The most general form for these quantities is

$$\mathcal{S}_{\sigma\lambda}^{(Q)} = v_\sigma \left[ \tau_1^{(Q)} v_\lambda + \tau_2^{(Q)} v'_\lambda + \tau_3^{(Q)} \gamma_\lambda \right] + \tau_4^{(Q)} g_{\sigma\lambda}. \quad (2.9)$$

The functions  $\tau_i$  depend on  $w$ , and have mass dimension one.<sup>3</sup> They are not all independent.

The equation of motion for the heavy quarks,  $(v \cdot D) h_v^{(Q)} = 0$ , implies

$$\begin{aligned} w \tau_1^{(c)} + \tau_2^{(c)} - \tau_3^{(c)} &= 0, \\ \tau_1^{(b)} + w \tau_2^{(b)} - \tau_3^{(b)} + \tau_4^{(b)} &= 0. \end{aligned} \quad (2.10)$$

Four more relations can be derived using

$$i \partial_\nu (\bar{h}_{v'}^{(c)} \Gamma h_v^{(b)}) = (\bar{\Lambda} v_\nu - \bar{\Lambda}' v'_\nu) \bar{h}_{v'}^{(c)} \Gamma h_v^{(b)}, \quad (2.11)$$

which is valid between the states destroyed by the fields in  $F_{v'}^\sigma$  and  $H_v$ . This relation follows from translation invariance and the definition of the heavy quark fields  $h_v^{(Q)}$ . It implies that

---

<sup>3</sup>Order  $\Lambda_{\text{QCD}}/m_c$  corrections were also analyzed in Ref. [20]. We find that  $\tau_4$  (denoted  $\xi_4$  in [20]) does contribute in Eq. (2.8) for  $\Gamma = \gamma_\lambda \tilde{\Gamma}$ , and corrections to the Lagrangian are parameterized by more functions than in [20].



$$\mathcal{S}_{\sigma\lambda}^{(c)} + \mathcal{S}_{\sigma\lambda}^{(b)} = (\bar{\Lambda}v_\lambda - \bar{\Lambda}'v'_\lambda)v_\sigma\tau. \quad (2.12)$$

Eq. (2.12) gives the following relations<sup>4</sup>

$$\begin{aligned} \tau_1^{(c)} + \tau_1^{(b)} &= \bar{\Lambda}\tau, \\ \tau_2^{(c)} + \tau_2^{(b)} &= -\bar{\Lambda}'\tau, \\ \tau_3^{(c)} + \tau_3^{(b)} &= 0, \\ \tau_4^{(c)} + \tau_4^{(b)} &= 0. \end{aligned} \quad (2.13)$$

These relations express the  $\tau_j^{(b)}$ 's in terms of the  $\tau_j^{(c)}$ 's. Furthermore, combining Eqs. (2.10) with (2.13) yields

$$\begin{aligned} \tau_3^{(c)} &= w\tau_1^{(c)} + \tau_2^{(c)}, \\ \tau_4^{(c)} &= (w-1)(\tau_1^{(c)} - \tau_2^{(c)}) - (w\bar{\Lambda}' - \bar{\Lambda})\tau. \end{aligned} \quad (2.14)$$

All order  $\Lambda_{\text{QCD}}/m_Q$  corrections to the form factors coming from the matching of the QCD currents onto those in the effective theory are expressible in terms of  $\bar{\Lambda}\tau$  and  $\bar{\Lambda}'\tau$  and two functions, which we take to be  $\tau_1^{(c)}$  and  $\tau_2^{(c)}$ . From Eqs. (2.8) and (2.9) it is evident that only  $\tau_4^{(Q)}$  can contribute at zero recoil. Eq. (2.14) determines this contribution in terms of  $\tau(1)$  and measurable mass splittings given in Eq. (1.10),

$$\tau_4^{(b)}(1) = -\tau_4^{(c)}(1) = (\bar{\Lambda}' - \bar{\Lambda})\tau(1). \quad (2.15)$$

Note that with our methods Eq. (2.15) cannot be derived working exclusively at zero recoil. At that kinematic point, matrix elements of the operator  $\bar{h}_v^{(c)}\Gamma h_v^{(b)}$  vanish between a  $B$  meson and an excited charmed meson, and so Eq. (2.11) only implies that  $\tau_4^{(c)} + \tau_4^{(b)} = 0$ . Eq. (2.15) relies on the assumption that the  $\tau_j^{(Q)}(w)$  are continuous at  $w = 1$ .

Next consider the terms originating from order  $\Lambda_{\text{QCD}}/m_Q$  corrections to the HQET Lagrangian,  $\delta\mathcal{L}$  in Eq. (1.4). These corrections modify the heavy meson states compared to their infinite heavy quark mass limit. For example, they cause the mixing of the  $D_1$  with the  $J^P = 1^+$  member of the  $s_l^{\pi_l} = \frac{1}{2}^+$  doublet. (This is a very small effect, since the  $D_1$  is not any broader than the  $D_2^*$ .) For matrix elements between the states destroyed by the fields in  $F_{v'}^\sigma$  and  $H_v$ , the time ordered products of the kinetic energy term in  $\delta\mathcal{L}$  with the leading order currents are

$$\begin{aligned} i \int d^4x T \left\{ O_{\text{kin},v'}^{(c)}(x) \left[ \bar{h}_{v'}^{(c)} \Gamma h_v^{(b)} \right] (0) \right\} &= \eta_{\text{ke}}^{(c)} \text{Tr} \left\{ v_\sigma \bar{F}_{v'}^\sigma \Gamma H_v \right\}, \\ i \int d^4x T \left\{ O_{\text{kin},v}^{(b)}(x) \left[ \bar{h}_{v'}^{(c)} \Gamma h_v^{(b)} \right] (0) \right\} &= \eta_{\text{ke}}^{(b)} \text{Tr} \left\{ v_\sigma \bar{F}_{v'}^\sigma \Gamma H_v \right\}. \end{aligned} \quad (2.16)$$

These corrections do not violate spin symmetry, so their contributions enter the same way as the  $m_Q \rightarrow \infty$  Isgur-Wise function,  $\tau$ .

---

<sup>4</sup>In Ref. [2] two out of these four relations were obtained (only those two were needed to get Eq. (2.15)). We thank M. Neubert for pointing out that there are two additional constraints.

For matrix elements between the states destroyed by the fields in  $F_v^\sigma$  and  $H_v$ , the time ordered products of the chromomagnetic term in  $\delta\mathcal{L}$  with the leading order currents are

$$\begin{aligned} i \int d^4x T \left\{ O_{\text{mag},v'}^{(c)}(x) \left[ \bar{h}_{v'}^{(c)} \Gamma h_v^{(b)} \right] (0) \right\} &= \text{Tr} \left\{ \mathcal{R}_{\sigma\alpha\beta}^{(c)} \bar{F}_{v'}^\sigma i\sigma^{\alpha\beta} \frac{1+\psi'}{2} \Gamma H_v \right\}, \\ i \int d^4x T \left\{ O_{\text{mag},v}^{(b)}(x) \left[ \bar{h}_{v'}^{(c)} \Gamma h_v^{(b)} \right] (0) \right\} &= \text{Tr} \left\{ \mathcal{R}_{\sigma\alpha\beta}^{(b)} \bar{F}_{v'}^\sigma \Gamma \frac{1+\psi'}{2} i\sigma^{\alpha\beta} H_v \right\}. \end{aligned} \quad (2.17)$$

The most general parameterizations of  $\mathcal{R}^{(Q)}$  are

$$\begin{aligned} \mathcal{R}_{\sigma\alpha\beta}^{(c)} &= \eta_1^{(c)} v_\sigma \gamma_\alpha \gamma_\beta + \eta_2^{(c)} v_\sigma v_\alpha \gamma_\beta + \eta_3^{(c)} g_{\sigma\alpha} v_\beta, \\ \mathcal{R}_{\sigma\alpha\beta}^{(b)} &= \eta_1^{(b)} v_\sigma \gamma_\alpha \gamma_\beta + \eta_2^{(b)} v_\sigma v'_\alpha \gamma_\beta + \eta_3^{(b)} g_{\sigma\alpha} v'_\beta. \end{aligned} \quad (2.18)$$

Only the part of  $\mathcal{R}_{\sigma\alpha\beta}^{(Q)}$  antisymmetric in  $\alpha$  and  $\beta$  contributes when inserted into Eq. (2.17). The functions  $\eta_i$  depend on  $w$ , and have mass dimension one. Note that  $g_{\sigma\alpha} \gamma_\beta$  is dependent on the tensor structures included in Eq. (2.18) for matrix elements between these states. For example, for the  $\Lambda_{\text{QCD}}/m_c$  corrections the following trace identity holds

$$\text{Tr} \left\{ \left[ v_\sigma \gamma_\alpha \gamma_\beta + 2g_{\sigma\alpha} v_\beta + 2(1+w) g_{\sigma\alpha} \gamma_\beta \right] \bar{F}_{v'}^\sigma \sigma^{\alpha\beta} \frac{1+\psi'}{2} \Gamma H_v \right\} = 0. \quad (2.19)$$

All contributions arising from the time ordered products in Eq. (2.17) vanish at zero recoil, since  $v_\sigma \bar{F}_v^\sigma = 0$  and  $v_\alpha (1+\psi') \sigma^{\alpha\beta} (1+\psi') = 0$ . Thus we find that at zero recoil the only  $\Lambda_{\text{QCD}}/m_Q$  corrections that contribute are determined by measured meson mass splittings and the value of the leading order Isgur-Wise function at zero recoil.

The form factors in Eq. (2.1) depend on  $\eta_i^{(b)}$  only through the linear combination  $\eta_b = \eta_{\text{ke}}^{(b)} + 6\eta_1^{(b)} - 2(w-1)\eta_2^{(b)} + \eta_3^{(b)}$ . Denoting  $\varepsilon_Q = 1/(2m_Q)$  and dropping the superscript on  $\tau_i^{(c)}$  and  $\eta_i^{(c)}$ , the  $B \rightarrow D_1 e \bar{\nu}_e$  form factors are [2]

$$\begin{aligned} \sqrt{6} f_A &= -(w+1)\tau - \varepsilon_b \{ (w-1)[(\bar{\Lambda}' + \bar{\Lambda})\tau - (2w+1)\tau_1 - \tau_2] + (w+1)\eta_b \} \\ &\quad - \varepsilon_c [4(w\bar{\Lambda}' - \bar{\Lambda})\tau - 3(w-1)(\tau_1 - \tau_2) + (w+1)(\eta_{\text{ke}} - 2\eta_1 - 3\eta_3)], \\ \sqrt{6} f_{V_1} &= (1-w^2)\tau - \varepsilon_b (w^2-1)[(\bar{\Lambda}' + \bar{\Lambda})\tau - (2w+1)\tau_1 - \tau_2 + \eta_b] \\ &\quad - \varepsilon_c [4(w+1)(w\bar{\Lambda}' - \bar{\Lambda})\tau - (w^2-1)(3\tau_1 - 3\tau_2 - \eta_{\text{ke}} + 2\eta_1 + 3\eta_3)], \\ \sqrt{6} f_{V_2} &= -3\tau - 3\varepsilon_b [(\bar{\Lambda}' + \bar{\Lambda})\tau - (2w+1)\tau_1 - \tau_2 + \eta_b] \\ &\quad - \varepsilon_c [(4w-1)\tau_1 + 5\tau_2 + 3\eta_{\text{ke}} + 10\eta_1 + 4(w-1)\eta_2 - 5\eta_3], \\ \sqrt{6} f_{V_3} &= (w-2)\tau + \varepsilon_b \{ (2+w)[(\bar{\Lambda}' + \bar{\Lambda})\tau - (2w+1)\tau_1 - \tau_2] - (2-w)\eta_b \} \\ &\quad + \varepsilon_c [4(w\bar{\Lambda}' - \bar{\Lambda})\tau + (2+w)\tau_1 + (2+3w)\tau_2 \\ &\quad + (w-2)\eta_{\text{ke}} - 2(6+w)\eta_1 - 4(w-1)\eta_2 - (3w-2)\eta_3]. \end{aligned} \quad (2.20)$$

The analogous formulae for  $B \rightarrow D_2^* e \bar{\nu}_e$  are

$$\begin{aligned} k_V &= -\tau - \varepsilon_b [(\bar{\Lambda}' + \bar{\Lambda})\tau - (2w+1)\tau_1 - \tau_2 + \eta_b] - \varepsilon_c (\tau_1 - \tau_2 + \eta_{\text{ke}} - 2\eta_1 + \eta_3), \\ k_{A_1} &= -(1+w)\tau - \varepsilon_b \{ (w-1)[(\bar{\Lambda}' + \bar{\Lambda})\tau - (2w+1)\tau_1 - \tau_2] + (1+w)\eta_b \} \\ &\quad - \varepsilon_c [(w-1)(\tau_1 - \tau_2) + (w+1)(\eta_{\text{ke}} - 2\eta_1 + \eta_3)], \\ k_{A_2} &= -2\varepsilon_c (\tau_1 + \eta_2), \\ k_{A_3} &= \tau + \varepsilon_b [(\bar{\Lambda}' + \bar{\Lambda})\tau - (2w+1)\tau_1 - \tau_2 + \eta_b] - \varepsilon_c (\tau_1 + \tau_2 - \eta_{\text{ke}} + 2\eta_1 - 2\eta_2 - \eta_3). \end{aligned} \quad (2.21)$$

Recall that  $f_{V_1}$  determines the zero recoil matrix elements of the weak currents. From Eqs. (2.20) it follows that

$$\sqrt{6} f_{V_1}(1) = -8 \varepsilon_c (\bar{\Lambda}' - \bar{\Lambda}) \tau(1). \quad (2.22)$$

The allowed kinematic range for  $B \rightarrow D_1 e \bar{\nu}_e$  decay is  $1 < w < 1.32$ , while for  $B \rightarrow D_2^* e \bar{\nu}_e$  decay it is  $1 < w < 1.31$ . Since these ranges are fairly small, and at zero recoil there are some constraints on the  $\Lambda_{\text{QCD}}/m_Q$  corrections, it is useful to consider the decay rates given in Eq. (2.2) expanded in powers of  $w - 1$ . The general structure of the expansion of  $d\Gamma/dw$  is elucidated schematically below,

$$\begin{aligned} \frac{d\Gamma_{D_1}^{(\lambda=0)}}{dw} &\sim \sqrt{w^2 - 1} \left[ (w - 1)^0 (0 + 0\varepsilon + \varepsilon^2 + \varepsilon^3 + \dots) \right. \\ &\quad \left. + (w - 1)^1 (0 + \varepsilon + \varepsilon^2 + \dots) + (w - 1)^2 (1 + \varepsilon + \dots) + \dots \right], \\ \frac{d\Gamma_{D_1}^{(|\lambda|=1)}}{dw} &\sim \sqrt{w^2 - 1} \left[ (w - 1)^0 (0 + 0\varepsilon + \varepsilon^2 + \varepsilon^3 + \dots) \right. \\ &\quad \left. + (w - 1)^1 (1 + \varepsilon + \dots) + (w - 1)^2 (1 + \varepsilon + \dots) + \dots \right], \\ \frac{d\Gamma_{D_2}^{(|\lambda|=0,1)}}{dw} &\sim (w^2 - 1)^{3/2} \left[ (w - 1)^0 (1 + \varepsilon + \dots) + (w - 1)^1 (1 + \varepsilon + \dots) + \dots \right]. \end{aligned} \quad (2.23)$$

Here  $\varepsilon^n$  denotes a term of order  $(\Lambda_{\text{QCD}}/m_Q)^n$ . The zeros in Eq. (2.23) are consequences of heavy quark symmetry, as the leading contribution to the matrix elements of the weak currents at zero recoil is of order  $\Lambda_{\text{QCD}}/m_Q$ . Thus, the  $D_1$  decay rate at  $w = 1$  starts out at order  $\Lambda_{\text{QCD}}^2/m_Q^2$ . Similarly, from Eq. (2.2) it is evident that the vanishing of  $f_{V_1}(1)$  in the  $m_Q \rightarrow \infty$  limit implies that at order  $w - 1$  the  $D_1^{(\lambda=0)}$  rate starts out at order  $\Lambda_{\text{QCD}}/m_Q$ . The  $D_2^*$  decay rate is suppressed by an additional power of  $w^2 - 1$ , so there is no further restriction on its structure.

In this paper we present predictions using two different approximations to the decay rates. In approximation A we treat  $w - 1$  as order  $\Lambda_{\text{QCD}}/m_Q$  and expand the decay rates in these parameters. In approximation B the known order  $\Lambda_{\text{QCD}}/m_Q$  contributions to the form factors are kept, as well as the full  $w$ -dependence of the decay rates.

Expanding the terms in the square brackets in Eq. (2.2) in powers of  $w - 1$  gives

$$\begin{aligned} \frac{d^2\Gamma_{D_1}}{dw d\cos\theta} &= \Gamma_0 \tau^2(1) r_1^3 \sqrt{w^2 - 1} \sum_n (w - 1)^n \left\{ \sin^2\theta s_1^{(n)} \right. \\ &\quad \left. + (1 - 2r_1 w + r_1^2) \left[ (1 + \cos^2\theta) t_1^{(n)} - 4 \cos\theta \sqrt{w^2 - 1} u_1^{(n)} \right] \right\}, \\ \frac{d^2\Gamma_{D_2^*}}{dw d\cos\theta} &= \frac{3}{2} \Gamma_0 \tau^2(1) r_2^3 (w^2 - 1)^{3/2} \sum_n (w - 1)^n \left\{ \frac{4}{3} \sin^2\theta s_2^{(n)} \right. \\ &\quad \left. + (1 - 2r_2 w + r_2^2) \left[ (1 + \cos^2\theta) t_2^{(n)} - 4 \cos\theta \sqrt{w^2 - 1} u_2^{(n)} \right] \right\}. \end{aligned} \quad (2.24)$$

(We do not expand the factors of  $\sqrt{w^2 - 1}$  that multiply  $\cos\theta$ ). The subscripts of the coefficients  $s, t, u$  denote the spin of the excited  $D$  meson, while the superscripts refer to the

order in the  $w - 1$  expansion. The  $u_i^{(n)}$  terms proportional to  $\cos \theta$  only affect the lepton spectrum, since they vanish when integrated over  $\theta$ .

Eqs. (2.2), (2.20), and (2.21) yield the following expressions for the coefficients in the  $D_1$  decay rate in Eq. (2.24),

$$\begin{aligned}
s_1^{(0)} &= 32\varepsilon_c^2 (1 - r_1)^2 (\bar{\Lambda}' - \bar{\Lambda})^2 + \dots, \\
s_1^{(1)} &= 32\varepsilon_c (1 - r_1^2) (\bar{\Lambda}' - \bar{\Lambda}) + \dots, \\
s_1^{(2)} &= 8(1 + r_1)^2 + \dots, \\
t_1^{(0)} &= 32\varepsilon_c^2 (\bar{\Lambda}' - \bar{\Lambda})^2 + \dots, \\
t_1^{(1)} &= 4 + 8\varepsilon_c [4(\bar{\Lambda}' - \bar{\Lambda}) + \hat{\eta}_{ke} - 2\hat{\eta}_1 - 3\hat{\eta}_3] + 8\varepsilon_b \hat{\eta}_b + \dots, \\
t_1^{(2)} &= 8(1 + \hat{\tau}') + \dots, \\
u_1^{(0)} &= 8\varepsilon_c (\bar{\Lambda}' - \bar{\Lambda}) + \dots, \\
u_1^{(1)} &= 2 + \dots.
\end{aligned} \tag{2.25}$$

For the decay rate into  $D_2^*$  the first two terms in the  $w - 1$  expansion are

$$\begin{aligned}
s_2^{(0)} &= 4(1 - r_2)^2 [1 + 2\varepsilon_b \hat{\eta}_b + 2\varepsilon_c (\hat{\eta}_{ke} - 2\hat{\eta}_1 + \hat{\eta}_3)] + \dots, \\
s_2^{(1)} &= 4(1 - r_2)^2 (1 + 2\hat{\tau}') + \dots, \\
t_2^{(0)} &= 4 + 8\varepsilon_b \hat{\eta}_b + 8\varepsilon_c (\hat{\eta}_{ke} - 2\hat{\eta}_1 + \hat{\eta}_3) + \dots, \\
t_2^{(1)} &= 2(3 + 4\hat{\tau}') + \dots, \\
u_2^{(0)} &= 2 + \dots.
\end{aligned} \tag{2.26}$$

In Eqs. (2.25) and (2.26) the functions  $\tau$ ,  $\tau' = d\tau/dw$ , and  $\eta_i$  are all evaluated at  $w = 1$ , and the functions with a hat are normalized to  $\tau(1)$  (e.g.,  $\hat{\eta}_i = \eta_i/\tau(1)$ ,  $\hat{\tau}' = \tau'/\tau(1)$ , etc.). The ellipses denote higher order terms in the  $\Lambda_{\text{QCD}}/m_Q$  expansion. The  $u_i^{(n)}$  terms are suppressed by  $\sqrt{w^2 - 1}$  compared to  $s_i^{(n)}$  and  $t_i^{(n)}$ , therefore we displayed the  $u$ 's to one lower order than the  $s$  and  $t$  coefficients. (Note that  $u_1^{(0)}$  also starts out at order  $\Lambda_{\text{QCD}}/m_Q$  as a consequence of the vanishing of  $f_{V_1}(1)$  in the  $m_Q \rightarrow \infty$  limit, as it was shown for  $s_1^{(1)}$  after Eq. (2.23).)

The order  $\Lambda_{\text{QCD}}/m_Q$  terms proportional to  $\bar{\Lambda}' - \bar{\Lambda}$  are very significant for the  $D_1$  decay rate. The decay rate into  $D_2^*$  does not receive a similarly large enhancement from order  $\Lambda_{\text{QCD}}/m_Q$  terms proportional to  $\bar{\Lambda}' - \bar{\Lambda}$ . The coefficients  $s_2^{(n)}$  and  $t_2^{(n)}$  are independent of  $\bar{\Lambda}'$  and  $\bar{\Lambda}$  to the order displayed in Eq. (2.26).

The values of  $s_1^{(0)}$  and  $t_1^{(0)}$  are known to order  $\Lambda_{\text{QCD}}^2/m_Q^2$ , and  $s_1^{(1)}$  and  $u_1^{(0)}$  are known to order  $\Lambda_{\text{QCD}}/m_Q$ . At order  $\Lambda_{\text{QCD}}/m_Q$ , the only unknowns in  $t_1^{(1)}$ ,  $s_2^{(0)}$ ,  $t_2^{(0)}$  are the  $\hat{\eta}_i$  functions that parameterize corrections to the HQET Lagrangian. The remaining coefficients in Eqs. (2.25) and (2.26) (i.e.,  $s_1^{(2)}$ ,  $t_1^{(2)}$ ,  $u_1^{(1)}$ ,  $s_2^{(1)}$ ,  $t_2^{(1)}$ ,  $u_2^{(0)}$ ) are known in the infinite mass limit in terms of  $\hat{\tau}'(1)$ , the slope of the  $m_Q \rightarrow \infty$  Isgur-Wise function at zero recoil. At order  $\Lambda_{\text{QCD}}/m_Q$ , these six coefficients depend on the unknown subleading  $\tau_i$  and  $\eta_i$  functions.

The values of  $\tau'$ ,  $\eta_i^{(Q)}$  and  $\tau_{1,2}$  that occur in Eqs. (2.25) and (2.26) are not known ( $\tau_i$  only appears in the terms replaced by ellipses).  $\eta_{1,2,3}^{(Q)}$ , which parameterize time ordered products

of the chromomagnetic operator, are expected to be small (compared to  $\Lambda_{\text{QCD}}$ ), and we neglect them hereafter. This is supported by the very small  $D_2^* - D_1$  mass splitting, and the fact that model calculations indicate that the analogous functions parameterizing time ordered products of the chromomagnetic operator for  $B \rightarrow D^{(*)} e \bar{\nu}_e$  decays are small [21]. On the other hand, there is no reason to expect  $\tau_{1,2}$  and  $\eta_{\text{ke}}^{(Q)}$  to be much smaller than about 500 MeV. Note that the large value for  $\lambda'_1$  is probably a consequence of the  $D_1$  and  $D_2^*$  being  $P$ -waves in the quark model, and does not necessarily imply that  $O_{\text{kin}}^{(Q)}$  significantly distorts the overlap of wave functions that yield  $\eta_{\text{ke}}^{(Q)}$ .

Even though  $\varepsilon_c(\bar{\Lambda}' - \bar{\Lambda}) \simeq 0.14$  is quite small, the order  $\Lambda_{\text{QCD}}/m_Q$  correction to  $t_1^{(1)}$  proportional to  $\varepsilon_c(\bar{\Lambda}' - \bar{\Lambda})$  is as large as the leading  $m_Q \rightarrow \infty$  contribution. This occurs because it has an anomalously large coefficient and does not necessarily mean that the  $\Lambda_{\text{QCD}}/m_Q$  expansion has broken down. For example, the part of the  $\Lambda_{\text{QCD}}^2/m_c^2$  corrections that involve  $\bar{\Lambda}'$ ,  $\bar{\Lambda}$ , and  $\tau'(1)$  affect  $s_1^{(1)}$  by  $(21 + 10\hat{\tau}')\%$ , and  $t_1^{(1)}$  by  $(44 + 15\hat{\tau}')\%$  (using  $\bar{\Lambda} = 0.4 \text{ GeV}$  [7]). These corrections follow from Eq. (2.20), but they are neglected in Eq. (2.25) (i.e., approximation A), because there are other order  $\Lambda_{\text{QCD}}^2/m_Q^2$  effects we have not calculated.

As the kinetic energy operator does not violate spin symmetry, effects of  $\eta_{\text{ke}}^{(Q)}$  can be absorbed into  $\tau$  by the replacement of  $\tau$  by  $\tilde{\tau} = \tau + \varepsilon_c \eta_{\text{ke}}^{(c)} + \varepsilon_b \eta_{\text{ke}}^{(b)}$ . This replacement introduces an error of order  $\Lambda_{\text{QCD}}^2/m_Q^2$ , in  $t_1^{(1)}$ , etc. But due to the presence of large  $\Lambda_{\text{QCD}}/m_Q$  corrections, the resulting  $\Lambda_{\text{QCD}}^2/m_Q^2$  error is also sizable, and is expected to be more like an order  $\Lambda_{\text{QCD}}/m_Q$  correction. Hereafter, unless explicitly stated otherwise, it is understood that the replacement  $\tau \rightarrow \tilde{\tau}$  is made. But we shall examine the sensitivity of our results to  $\eta_{\text{ke}}$  (assuming it has the same shape as  $\tau$ ).

In approximation A we treat  $w - 1$  as order  $\Lambda_{\text{QCD}}/m_Q$  [2], and keep terms up to order  $(\Lambda_{\text{QCD}}/m_Q)^{2-n}$  in  $s_1^{(n)}$  and  $t_1^{(n)}$  ( $n = 0, 1, 2$ ) in Eq. (2.25), and up to order  $(\Lambda_{\text{QCD}}/m_Q)^{1-n}$  in  $s_2^{(n)}$  and  $t_2^{(n)}$  ( $n = 0, 1$ ) in Eq. (2.26). Since the  $u_i^{(n)}$  are suppressed by  $\sqrt{w^2 - 1}$  compared to  $s_i^{(n)}$  and  $t_i^{(n)}$ , we keep  $u_i^{(n)}$  to one lower order than the  $s$  and  $t$  coefficients, i.e., to order  $(\Lambda_{\text{QCD}}/m_Q)^{1-n}$  ( $n = 0, 1$ ) for  $B \rightarrow D_1$  decay and order  $(\Lambda_{\text{QCD}}/m_Q)^n$  ( $n = 0$ ) for  $B \rightarrow D_2^*$  decay. The terms included in approximation A are precisely the ones explicitly shown in Eqs. (2.25) and (2.26). This power counting has the advantage that the unknown functions,  $\tau_1$  and  $\tau_2$ , do not enter the predictions.<sup>5</sup> Neglecting higher order terms in the  $w - 1$  expansion in approximation A gives rise to a sizable error for the  $B \rightarrow D_1 e \bar{\nu}_e$  decay<sup>6</sup>. The order  $(w - 1)^3$  term is important for the decay into helicity zero  $D_1$  in the  $m_Q \rightarrow \infty$  limit, since the helicity zero rate (which, as we shall see, dominates over the helicity one rate) starts out at order  $(w - 1)^2$  as shown in Eq. (2.23).

In approximation B we do not expand the decay rates in powers of  $w - 1$ . We keep the

---

<sup>5</sup>Approximation A differs from our discussion in Ref. [2] only in the separation of the different helicity states of the excited charmed mesons, and keeping the  $1 - 2rw + r^2$  factors for the helicity one states as well as the  $(w^2 - 1)^{3/2}$  terms for the  $D_2^*$  rates unexpanded.

<sup>6</sup>We thank A. Le Yaouanc for pointing out the importance of these terms.

$\Lambda_{\text{QCD}}/m_Q$  corrections to the form factors that involve  $\bar{\Lambda}'$  and  $\bar{\Lambda}$  and examine the sensitivity of our results to the corrections involving  $\tau_1$  and  $\tau_2$  (assuming that they have the same shape as  $\tau$ , which is not a strong assumption). This approximation retains some order  $\Lambda_{\text{QCD}}^2/m_Q^2$  terms away from zero recoil in the differential decay rates. Furthermore, a linear form for the Isgur-Wise function is assumed,  $\tau(w) = \tau(1) [1 + \hat{\tau}'(w-1)]$ . The uncertainty in the  $\Lambda_{\text{QCD}}/m_Q$  corrections is parameterized by the functions  $\tau_{1,2}(w)$ . A different choice of  $\tau_{1,2}(w)$  changes what is retained by terms involving  $\bar{\Lambda}/m_Q$  and  $\bar{\Lambda}'/m_Q$ . In an approximation, which we shall refer to as B<sub>1</sub>, we set  $\tau_1 = \tau_2 = 0$  in Eqs. (2.20) and (2.21). (This is identical to saturating the first two relations in Eq. (2.13) by  $\tau_{1,2}^{(b)}$ , i.e., setting  $\tau_1^{(b)} = \bar{\Lambda} \tau$  and  $\tau_2^{(b)} = -\bar{\Lambda}' \tau$ .) An equally reasonable approximation, which we refer to as B<sub>2</sub>, is given by setting  $\tau_1 = \bar{\Lambda} \tau$  and  $\tau_2 = -\bar{\Lambda}' \tau$  in Eqs. (2.20) and (2.21). (This is identical to setting  $\tau_{1,2}^{(b)} = 0$ .) If the first two relations in Eq. (2.13) are taken as hints to the signs of  $\tau_1$  and  $\tau_2$ , then the difference between approximations B<sub>1</sub> and B<sub>2</sub> gives a rough estimate of the uncertainty related to the unknown  $\Lambda_{\text{QCD}}/m_Q$  corrections. When our predictions are sensitive to  $\tau_1$  and  $\tau_2$ , we shall vary these in a range larger than that spanned by approximations B<sub>1</sub> and B<sub>2</sub>. Note that the infinite mass limits of B<sub>1</sub> and B<sub>2</sub> coincide. Predictions of approximation A are within the spread of the approximation B results, except for those that depend on the helicity zero  $D_1$  rate. In that case, including the order  $(w-1)^3$  term in the infinite mass limit alone,  $s_1^{(3)} = 8(1+r_1)^2(1+2\hat{\tau}')$ , would bring the approximation A results close to approximation B.

Eqs. (2.25) and (2.26) show that the heavy quark expansion for  $B$  decays into excited charmed mesons is controlled by the excitation energies of the hadrons,  $\bar{\Lambda}'$  and  $\bar{\Lambda}$ . For highly excited mesons that have  $\bar{\Lambda}'$  comparable to  $m_c$ , the  $1/m_Q$  expansion is not useful. For the  $s_\ell^{\pi\ell} = \frac{3}{2}^+$  doublet  $\varepsilon_c \bar{\Lambda}' \sim 0.3$ . However, near zero recoil only  $\varepsilon_c (\bar{\Lambda}' - \bar{\Lambda}) \sim 0.14$  occurs at order  $\Lambda_{\text{QCD}}/m_Q$ .

The expressions for the decay rates in terms of form factors in Eq. (2.2) imply that one form factor dominates each decay rate near zero recoil, independent of the helicity of the  $D_1$  or  $D_2^*$  ( $f_{V_1}$  for  $D_1$  and  $k_{A_1}$  for  $D_2^*$ ). Thus, to all orders in the  $\Lambda_{\text{QCD}}/m_Q$  expansion,  $s_1^{(0)}/t_1^{(0)} = (1-r_1)^2$ , and  $s_2^{(0)}/t_2^{(0)} = (1-r_2)^2$ . This implies that for  $B \rightarrow D_1$  decay  $\lim_{w \rightarrow 1} \left[ (d\Gamma_{D_1}^{(\lambda=0)}/dw) / (d\Gamma_{D_1}^{(|\lambda|=1)}/dw) \right] = 1/2$ , and for  $B \rightarrow D_2^*$  decay  $\lim_{w \rightarrow 1} \left[ (d\Gamma_{D_2^*}^{(\lambda=0)}/dw) / (d\Gamma_{D_2^*}^{(|\lambda|=1)}/dw) \right] = 2/3$ . Note that the first of these ratios would vanish if the rates were calculated in the  $m_Q \rightarrow \infty$  limit. In that case  $f_{V_1}(1) = 0$ , so the ratio of helicity zero and helicity one  $B \rightarrow D_1$  rates is determined by the other form factors at zero recoil.

## A. Predictions

The relationship between  $s_1^{(0)}$  and  $s_1^{(1)}$  implies a model independent prediction for the slope parameter of semileptonic  $B$  decay into helicity zero  $D_1$ . This holds independent of the subleading Isgur-Wise functions that arise at order  $\Lambda_{\text{QCD}}/m_Q$ . The semileptonic decay rate to a helicity zero  $D_1$  meson is

$$\frac{d\Gamma_{D_1}^{(\lambda=0)}}{dw} = \frac{128}{3} \Gamma_0 r_1^3 (1-r_1)^2 \sqrt{w^2-1} \tau^2(1) \varepsilon_c^2 (\bar{\Lambda}' - \bar{\Lambda})^2 \left[ 1 - \rho_{D_1}^2 (w-1) + \dots \right], \quad (2.27)$$

Approximation	$R = \Gamma_{D_2^*}/\Gamma_{D_1}$	$\Gamma_{D_1}^{(\lambda=0)}/\Gamma_{D_1}$	$\Gamma_{D_2^*}^{(\lambda=0)}/\Gamma_{D_2^*}$	$\tau(1) \left[ \frac{6.0 \times 10^{-3}}{\mathcal{B}(B \rightarrow D_1 e \bar{\nu}_e)} \right]^{1/2}$
A <sub>∞</sub>	0.93	0.88	0.64	0.92
B <sub>∞</sub>	1.65	0.80	0.66	1.24
A	0.40	0.81	0.64	0.60
B <sub>1</sub>	0.52	0.72	0.63	0.71
B <sub>2</sub>	0.67	0.77	0.64	0.75

TABLE II. Predictions for various ratios of  $B \rightarrow D_1 e \bar{\nu}_e$  and  $B \rightarrow D_2^* e \bar{\nu}_e$  decay rates, as described in the text. The extracted value of  $\tau(1)$  is also shown. A<sub>∞</sub> and B<sub>∞</sub> denote the  $m_Q \rightarrow \infty$  limits of approximations A and B. These results correspond to  $\hat{\tau}' = \tau'(1)/\tau(1) = -1.5$ .

where the slope parameter  $\rho_{D_1}^2$  for helicity zero  $D_1$  has the value

$$\rho_{D_1}^2 = -\frac{1+r_1}{1-r_1} \frac{2m_c}{\bar{\Lambda}' - \bar{\Lambda}} + \mathcal{O}(1). \quad (2.28)$$

Since the decay rate at zero recoil is suppressed,  $\rho_{D_1}^2$  is of order  $m_Q/\Lambda_{\text{QCD}}$ . Note that this slope parameter is negative.

Recently the ALEPH [15] and CLEO [16] Collaborations measured, with some assumptions, the  $B \rightarrow D_1 e \bar{\nu}_e$  branching ratio. The average of their results is

$$\mathcal{B}(B \rightarrow D_1 e \bar{\nu}_e) = (6.0 \pm 1.1) \times 10^{-3}. \quad (2.29)$$

The  $B \rightarrow D_2^* e \bar{\nu}_e$  branching ratio has not yet been measured; CLEO set the limit  $\mathcal{B}(B \rightarrow D_2^* e \bar{\nu}_e) < 1\%$  [16], while ALEPH found  $\mathcal{B}(B \rightarrow D_2^* e \bar{\nu}_e) < 0.2\%$  [15].

Predictions for various quantities of experimental interest are made in Table II using  $\bar{\Lambda}' - \bar{\Lambda} = 0.39 \text{ GeV}$ ,  $\bar{\Lambda} = 0.4 \text{ GeV}$ ,  $\tau_B = 1.6 \text{ ps}$ ,  $|V_{cb}| = 0.04$ ,  $m_c = 1.4 \text{ GeV}$ ,  $m_b = 4.8 \text{ GeV}$ . Keeping  $m_b - m_c$  fixed and varying  $m_c$  by  $\pm 0.1 \text{ GeV}$  only affects our results at the few percent level. These predictions depend on the shape of the Isgur-Wise function. In our approximations this enters through the slope parameter,  $\hat{\tau}' = \tau'(1)/\tau(1)$ , which is expected to be of order  $-1$ . We shall quote results for the “central value”  $\hat{\tau}' = -1.5$ , motivated by model predictions [22–25], and discuss the sensitivity to this assumption. For  $B \rightarrow D_1 e \bar{\nu}_e$  decay we use  $r_1 = 0.459$  and  $1 < w < 1.319$ , whereas for  $B \rightarrow D_2^* e \bar{\nu}_e$  decay  $r_2 = 0.466$  and  $1 < w < 1.306$ .

The order  $\Lambda_{\text{QCD}}/m_Q$  corrections are important for predicting

$$R \equiv \frac{\mathcal{B}(B \rightarrow D_2^* e \bar{\nu}_e)}{\mathcal{B}(B \rightarrow D_1 e \bar{\nu}_e)}. \quad (2.30)$$

In the  $m_Q \rightarrow \infty$  limit  $R \simeq 1.65$  for  $\hat{\tau}' = -1.5$  (this is the B<sub>∞</sub> result in Table II). The sizable difference between approximations A and B is mainly due to the order  $(w-1)^3$  contribution to the helicity zero  $D_1$  rate. For  $\hat{\tau}' = -1.5$  this term by itself would shift the approximation A result for  $R$  from 0.40 to 0.49 and the A<sub>∞</sub> prediction from 0.93 to 1.65. The  $\Lambda_{\text{QCD}}/m_Q$  correction to the form factors yield a large suppression of  $R$  as shown in Table II and Fig. 1a. Fig. 1a also shows that  $R$  is fairly insensitive to  $\hat{\tau}'$ . The difference of the B<sub>1</sub> and B<sub>2</sub> results in

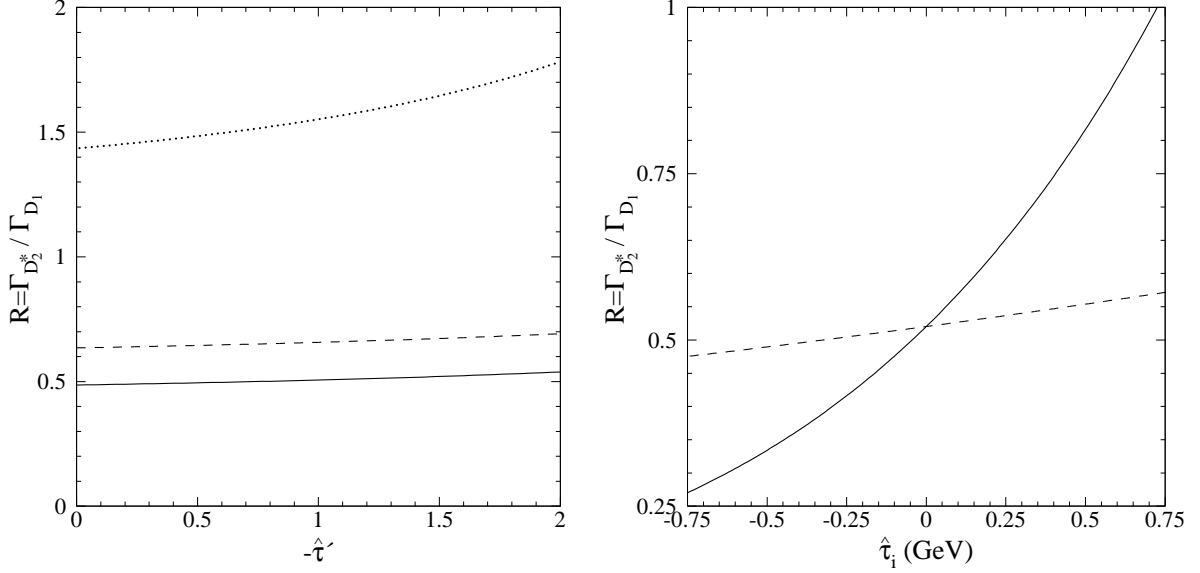


FIG. 1. Fig. 1a shows  $R = \mathcal{B}(B \rightarrow D_2^* e \bar{\nu}_e) / \mathcal{B}(B \rightarrow D_1 e \bar{\nu}_e)$  as a function of  $\hat{\tau}'$ . The dotted curve is the  $m_Q \rightarrow \infty$  limit ( $B_\infty$ ), solid curve is approximation  $B_1$ , dashed curve is  $B_2$ . Fig. 1b shows  $R$  as a function of  $\hat{\tau}_1 (= \tau_1 / \tau)$  for  $\hat{\tau}_2 = 0$  (solid curve), and as a function of  $\hat{\tau}_2$  for  $\hat{\tau}_1 = 0$  (dashed curve). Note that the scales in Fig. 1a and 1b are different.

Table II and Fig. 1a shows that  $R$  is sensitive to the unknown  $\Lambda_{\text{QCD}}/m_Q$  corrections,  $\tau_1$  and  $\tau_2$ . In Fig. 1b we plot  $R$  in approximation B as a function of  $\hat{\tau}_1$  setting  $\hat{\tau}_2 = 0$  (solid curve), and as a function of  $\hat{\tau}_2$  setting  $\hat{\tau}_1 = 0$  (dashed curve). Fig. 1b shows that  $R$  is fairly insensitive to  $\tau_2$ , whereas it depends sensitively on  $\tau_1$ . In the range  $-0.75 \text{ GeV} < \hat{\tau}_1 < 0.75 \text{ GeV}$ ,  $R$  goes over  $0.27 < R < 1.03$ . This suppression of  $R$  compared to the infinite mass limit is supported by the experimental data. (It is possible that part of the reason for the strong ALEPH bound  $\mathcal{B}(B \rightarrow D_2^* e \bar{\nu}_e X) \times \mathcal{B}(D_2^* \rightarrow D^{(*)}\pi) \lesssim (1.5 - 2.0) \times 10^{-3}$  [15] is a suppression of  $\mathcal{B}(D_2^* \rightarrow D^{(*)}\pi)$  compared to  $\mathcal{B}(D_1 \rightarrow D^*\pi)$ .)

The prediction for the fraction of helicity zero  $D_1$ 's in semileptonic  $B \rightarrow D_1$  decay,  $\Gamma_{D_1}^{(\lambda=0)} / \Gamma_{D_1}$ , is surprisingly stable in the different approximations (see Table II). The weak dependence of this ratio on  $\hat{\tau}'$  is well described in approximation B for  $|1.5 + \hat{\tau}'| < 1$  by adding  $0.05(1.5 + \hat{\tau}')$ . The dependence on  $\tau_1$  is at the 0.01 level, while the  $\tau_2$ -dependence is  $-0.07 \hat{\tau}_2 / \text{GeV}$ . This is why the  $B_2$  result for this quantity is 0.05 larger than the  $B_1$  prediction. A linear dependence of  $(d\Gamma_{D_1}^{(\lambda=0)} / dw) / (d\Gamma_{D_1} / dw)$  on  $w$  between  $\lim_{w \rightarrow 1} [(d\Gamma_{D_1}^{(\lambda=0)} / dw) / (d\Gamma_{D_1} / dw)] = 1/3$  and  $[(d\Gamma_{D_1}^{(\lambda=0)} / dw) / (d\Gamma_{D_1} / dw)] = 1$  at  $w = w_{\text{max}}$  is consistent with our result.

A similar prediction exists for the fraction of helicity zero  $D_2^*$ 's in semileptonic  $B \rightarrow D_2^*$  decay. As can be seen from Table II, it is again quite stable. The dependence on  $\hat{\tau}'$  in approximation B is given by adding  $0.04(1.5 + \hat{\tau}')$ . However,  $\Gamma_{D_2^*}^{(\lambda=0)} / \Gamma_{D_2^*}$  is sensitive to both  $\tau_1$  and  $\tau_2$  at the (10–20)% level, and the small difference between the  $B_1$  and  $B_2$  predictions for this quantity in Table II is due to an accidental cancellation. The prediction for the  $w$  dependence of  $(d\Gamma_{D_2^*}^{(\lambda=0)} / dw) / (d\Gamma_{D_2^*} / dw)$  between  $\lim_{w \rightarrow 1} [(d\Gamma_{D_2^*}^{(\lambda=0)} / dw) / (d\Gamma_{D_2^*} / dw)] = 2/5$  and  $[(d\Gamma_{D_2^*}^{(\lambda=0)} / dw) / (d\Gamma_{D_2^*} / dw)] = 1$  at  $w = w_{\text{max}}$  in this case is not linear.



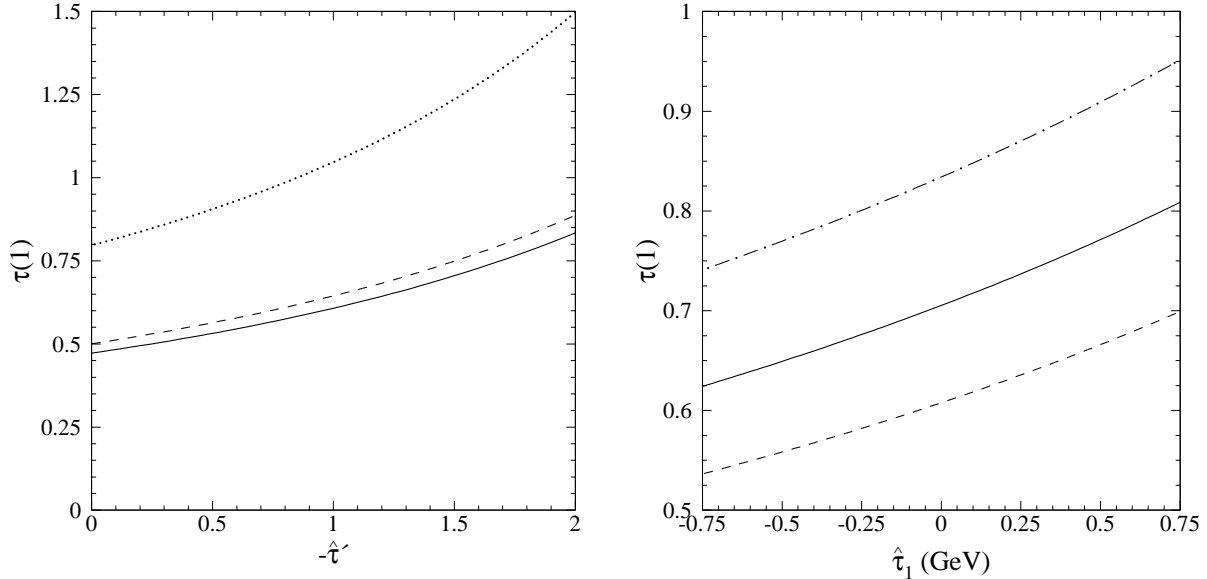


FIG. 2. Fig. 2a shows the extracted value of  $\tau(1)$  as a function of  $\hat{\tau}'$  in approximations  $B_\infty$ ,  $B_1$ , and  $B_2$ . The notation is the same as in Fig. 1. Fig. 2b shows the dependence of  $\tau(1)$  on  $\hat{\tau}_1$  for  $\hat{\tau}' = -1$  (dashed curve),  $\hat{\tau}' = -1.5$  (solid curve),  $\hat{\tau}' = -2$  (dash-dotted curve).

The predictions considered so far do not depend on the value of  $\tau(1)$ , but  $\tau(1)$  affects some results that we discuss later.  $\tau(1)$  can be determined from the measured  $B \rightarrow D_1 e \bar{\nu}_e$  branching ratio using the expressions in Eq. (2.24) and (2.25). Using approximation  $B_1$  and  $\hat{\tau}' = -1.5$ , we obtain

$$\tau(1) \left[ \frac{6.0 \times 10^{-3}}{\mathcal{B}(B \rightarrow D_1 e \bar{\nu}_e)} \right]^{1/2} = 0.71. \quad (2.31)$$

The extracted value of  $\tau(1)$  is plotted in Fig. 2a in approximations  $B_\infty$ ,  $B_1$ , and  $B_2$  as functions of  $\hat{\tau}'$ . The suppression of  $\tau(1)$  compared to the infinite mass limit indicates that the order  $\Lambda_{\text{QCD}}/m_Q$  corrections enhance the semileptonic  $B \rightarrow D_1$  width by about a factor of three. In approximation B the value of  $\tau(1)$  changes by less than 0.01 as  $\tau_2$  is varied in the range  $-0.75 \text{ GeV} < \hat{\tau}_2 < 0.75 \text{ GeV}$ , but  $\tau(1)$  is sensitive to  $\tau_1$  at the 15% level. In Fig. 2b we plot  $\tau(1)$  as a function of  $\hat{\tau}_1$  for  $\hat{\tau}' = -1$  (dashed curve),  $\hat{\tau}' = -1.5$  (solid curve), and  $\hat{\tau}' = -2$  (dash-dotted curve). For  $\tau_1 > 0$  (such as approximation  $B_2$ )  $\tau(1)$  is enhanced compared to the  $B_1$  value of 0.71.

The value of  $\tau(1)$  in approximation B is larger than that in approximation A. Most of the difference arises from the inclusion of the order  $(w-1)^3$  term,  $s_1^{(3)}$ , which reduces the theoretical expression for the helicity zero  $B \rightarrow D_1 e \bar{\nu}_e$  rate (for  $\hat{\tau}' < -0.5$ ), resulting in an increase in the value of  $\tau(1)$  needed to accommodate the measured rate. For  $\hat{\tau}' = -1.5$  this term by itself would shift the approximation A result from 0.60 to 0.66, and the  $A_\infty$  prediction from 0.92 to 1.22. The ISGW nonrelativistic constituent quark model predicts  $\tau(1) = 0.54$ , in rough agreement with Eq. (2.31) [22,19]. (For some other quark model predictions, see, e.g., Ref. [24,25]. QCD sum rules can also be used to estimate  $\tau$ , see, e.g., Ref [23].)

Approximation	$\delta(\Gamma_{D_2^*}/\Gamma_{D_1})$	$\delta(\Gamma_{D_1}^{(\lambda=0)}/\Gamma_{D_1})$	$\delta(\Gamma_{D_2^*}^{(\lambda=0)}/\Gamma_{D_2^*})$	$\delta\tau(1) \left[ \frac{6.0 \times 10^{-3}}{\mathcal{B}(B \rightarrow D_1 e \bar{\nu}_e)} \right]^{1/2}$
A <sub>∞</sub>	-0.68	0.10	0.02	-0.26
B <sub>∞</sub>	-1.63	0.19	-0.003	-0.32
A	-0.22	0.04	0.05	-0.24
B <sub>1</sub>	-0.55	0.06	-0.02	-0.32
B <sub>2</sub>	-0.68	0.07	-0.05	-0.33

TABLE III. Order  $\alpha_s$  and  $\alpha_s(\Lambda_{\text{QCD}}/m_Q)$  corrections to the predictions in Table II for  $\hat{\tau}' = -1.5$ . These numbers should be multiplied by  $\alpha_s(\sqrt{m_c m_b})/\pi$  to get the corrections to Table II.

The ALEPH and CLEO analyses that yield Eq. (2.29) assume that  $B \rightarrow D_1 e \bar{\nu}_e X$  is dominated by  $B \rightarrow D_1 e \bar{\nu}_e$ , and that  $D_1$  decays only into  $D^* \pi$ . If the first assumption turns out to be false then  $\tau(1)$  will decrease, if the second assumption is false then  $\tau(1)$  will increase compared to Eq. (2.31).

The predictions discussed above would change if we had not absorbed into  $\tau$  the time ordered product involving the kinetic energy operator. As discussed earlier (in the paragraph preceding the description of approximation A), the replacement of  $\tau$  by  $\tilde{\tau} = \tau + \varepsilon_c \eta_{\text{ke}}^{(c)} + \varepsilon_b \eta_{\text{ke}}^{(b)}$  introduces an error, which is formally of order  $\Lambda_{\text{QCD}}^2/m_Q^2$ . Absorbing  $\eta_{\text{ke}}$  into  $\tau$  almost fully eliminates the  $\eta_{\text{ke}}$  dependence of the  $D_2^*$  rate. For the  $D_1$  rate, however, absorbing  $\eta_{\text{ke}}$  into  $\tau$  generates at order  $\Lambda_{\text{QCD}}^2/m_Q^2$  a formally suppressed but numerically sizable  $\eta_{\text{ke}}$  dependence. This  $\eta_{\text{ke}}$  dependence is more like a typical  $\Lambda_{\text{QCD}}/m_Q$  correction, since the  $\Lambda_{\text{QCD}}/m_Q$  current corrections are as important as the infinite mass limit for the  $D_1$  rate. Keeping  $\hat{\eta}_{\text{ke}}^{(Q)} = \eta_{\text{ke}}^{(Q)}/\tau$  explicit in the results, the total  $B \rightarrow D_1$  semileptonic rate in units of  $\Gamma_0 \tau^2(1)$  is  $0.033 (1 + 1.1 \varepsilon_c \hat{\eta}_{\text{ke}}^{(c)} + \dots)$ , while the  $B \rightarrow D_2^*$  rate is  $0.017 (1 + 2.0 \varepsilon_c \hat{\eta}_{\text{ke}}^{(c)} + \dots)$ . From these expressions it is evident that, for  $-0.75 \text{ GeV} < \hat{\eta}_{\text{ke}} < 0.75 \text{ GeV}$ ,  $\tau(1)$  changes only by  $\pm 15\%$ , while  $R$  has a larger variation. In the future this uncertainty will be reduced if differential spectra can also be measured besides total rates in  $B \rightarrow D_1, D_2^*$  decays. Note that  $\eta_{\text{ke}}$  does not enter into predictions for the  $B \rightarrow D_1 e \bar{\nu}_e$  decay rate near zero recoil.

Order  $\alpha_s$  corrections to the results of this section can be calculated in a straightforward way, using well-known methods. Details of this calculation are given in Appendix A. The order  $\alpha_s$  corrections to the results shown in Table II are given in Table III. These are smaller than the uncertainty in our results from higher order terms in the  $\Lambda_{\text{QCD}}/m_Q$  expansion that have been neglected. The corrections are most significant for  $R = \Gamma_{D_2^*}/\Gamma_{D_1}$  and  $\tau(1)$  in approximation B; the central values of these quantities are reduced by about 9% and 4%, respectively. Some of these  $\alpha_s$  corrections depend sensitively on  $\hat{\tau}'$ , but they remain small for  $0 > \hat{\tau}' > -2$ . For the remainder of this paper, we neglect the small  $\alpha_s$  corrections.

Our predictions for the single differential  $B \rightarrow (D_1, D_2^*) e \bar{\nu}_e$  spectra follow from Eqs. (2.24), (2.25), and (2.26).  $d\Gamma/dw$  is given by integrating Eqs. (2.24) over  $d\cos\theta$ . This amounts to the replacements  $\sin^2\theta \rightarrow 4/3$ ,  $(1 + \cos^2\theta) \rightarrow 8/3$ , and  $\cos\theta \rightarrow 0$ . Thus  $d\Gamma/dw$  is trivial to obtain using either approximations A or B. The electron energy spectra are obtained by expressing  $\cos\theta$  in terms of  $y$  (where  $y = 2E_e/m_B$  is the rescaled electron energy) using Eq. (2.3), and integrating  $w$  over  $[(1-y)^2 + r^2]/[(2r(1-y)) < w < (1+r^2)/(2r)]$ . They

depend on the coefficients  $u_i^{(n)}$  which did not enter our results so far.

In Fig. 3 the electron spectrum for  $B \rightarrow D_1 e \bar{\nu}_e$  is plotted in units of  $\Gamma_0 \tau^2(1)$ . Figs. 3a and 3b are the spectra for helicity zero and helicity one  $D_1$ , respectively. In these plots  $\hat{\tau}' = -1.5$ . The dotted curve shows the  $m_Q \rightarrow \infty$  limit ( $B_\infty$ ), the solid curve is approximation  $B_1$ , the dashed curve is  $B_2$ . Note that the kinematic range for  $y$  is  $0 < y < 1 - r^2$ . Near  $y = 0$  and  $y = 1 - r^2$  the spectrum is dominated by contributions from  $w$  near  $w_{\max}$ . In this case, we expect sizable uncertainties in our results, for example, from unknown terms that occur in the  $u_i^{(n)}$  terms in Eq. (2.25) at a lower order than in the  $s$  and  $t$  coefficients. Fig. 3 shows the large enhancement of the  $D_1$  rate due to order  $\Lambda_{\text{QCD}}/m_Q$  corrections, and that the difference between approximations  $B_1$  and  $B_2$  is small compared to this enhancement. In Figs. 4a and 4b we plot the electron spectrum for  $B \rightarrow D_2^* e \bar{\nu}_e$  for helicity zero and helicity one  $D_2^*$ , respectively. In this case the  $\Lambda_{\text{QCD}}/m_Q$  corrections are less important.

### III. $B \rightarrow D_0^* e \bar{\nu}_e$ AND $B \rightarrow D_1^* e \bar{\nu}_e$ DECAYS

The other low lying states above the  $D^{(*)}$  ground states occur in a doublet with  $s_l^{\pi l} = \frac{1}{2}^+$ . These states are expected to be broad since they can decay into  $D^{(*)} \pi$  in an  $S$ -wave, unlike the  $D_1$  and  $D_2^*$  which can only decay in a  $D$ -wave. (An  $S$ -wave decay amplitude for the  $D_1$  is forbidden by heavy quark spin symmetry [3].) This section repeats the analysis of the previous section for these states. Since the notation, methods, and results are similar to those used in Sec. II, the discussion here will be briefer.

The matrix elements of the vector and axial currents between  $B$  mesons and  $D_0^*$  or  $D_1^*$  mesons can be parameterized by

$$\begin{aligned}
\langle D_0^*(v') | V^\mu | B(v) \rangle &= 0, \\
\frac{\langle D_0^*(v') | A^\mu | B(v) \rangle}{\sqrt{m_{D_0^*} m_B}} &= g_+ (v^\mu + v'^\mu) + g_- (v^\mu - v'^\mu), \\
\frac{\langle D_1^*(v', \epsilon) | V^\mu | B(v) \rangle}{\sqrt{m_{D_1^*} m_B}} &= g_{V_1} \epsilon^{*\mu} + (g_{V_2} v^\mu + g_{V_3} v'^\mu) (\epsilon^* \cdot v), \\
\frac{\langle D_1^*(v', \epsilon) | A^\mu | B(v) \rangle}{\sqrt{m_{D_1^*} m_B}} &= i g_A \epsilon^{\mu\alpha\beta\gamma} \epsilon_\alpha^* v_\beta v'_\gamma,
\end{aligned} \tag{3.1}$$

where  $g_i$  are functions of  $w$ . At zero recoil the matrix elements are determined by  $g_+(1)$  and  $g_{V_1}(1)$ . In terms of these form factors the double differential decay rates for  $B \rightarrow D_0^* e \bar{\nu}_e$  and  $B \rightarrow D_1^* e \bar{\nu}_e$  decays are

$$\begin{aligned}
\frac{d^2\Gamma_{D_0^*}}{dw d\cos\theta} &= 3\Gamma_0 r_0^{*3} (w^2 - 1)^{3/2} \sin^2\theta \left[ (1 + r_0^*) g_+ - (1 - r_0^*) g_- \right]^2, \\
\frac{d^2\Gamma_{D_1^*}}{dw d\cos\theta} &= 3\Gamma_0 r_1^{*3} \sqrt{w^2 - 1} \left\{ \sin^2\theta \left[ (w - r_1^*) g_{V_1} + (w^2 - 1)(g_{V_3} + r_1^* g_{V_2}) \right]^2 \right. \\
&\quad \left. + (1 - 2r_1^* w + r_1^{*2}) \left[ (1 + \cos^2\theta) [g_{V_1}^2 + (w^2 - 1)g_A^2] - 4\cos\theta \sqrt{w^2 - 1} g_{V_1} g_A \right] \right\}.
\end{aligned} \tag{3.2}$$

where  $\Gamma_0 = G_F^2 |V_{cb}|^2 m_B^5 / (192\pi^3)$ ,  $r_0^* = m_{D_0^*} / m_B$  and  $r_1^* = m_{D_1^*} / m_B$ .

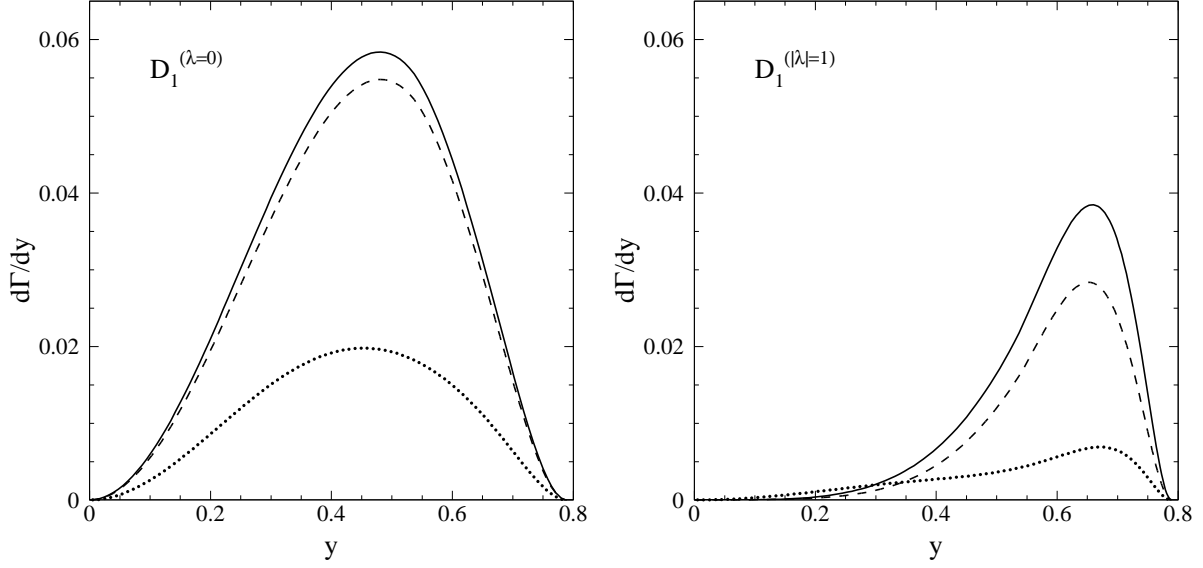


FIG. 3. Electron spectrum for  $B \rightarrow D_1 e \bar{\nu}_e$  in units of  $\Gamma_0 \tau^2(1)$  for  $\hat{\tau}' = -1.5$ . Figs. 3a and 3b are the spectra for helicity zero and helicity one  $D_1$ , respectively. Dotted curves show the  $m_Q \rightarrow \infty$  limit ( $B_\infty$ ), solid curves are approximation  $B_1$ , dashed curves are  $B_2$ .

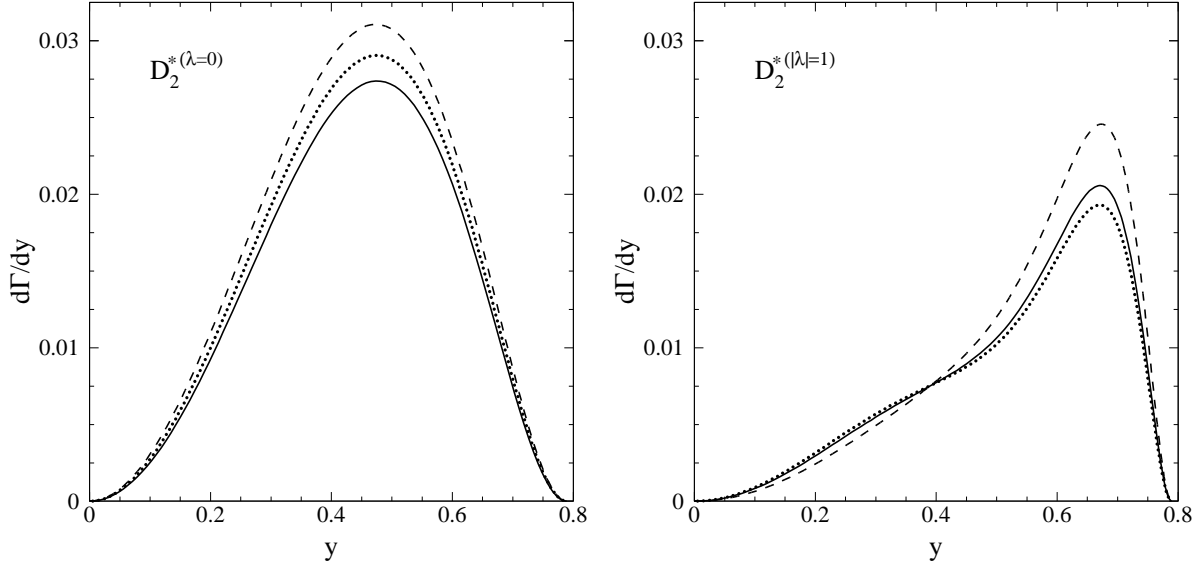


FIG. 4. Electron spectrum for  $B \rightarrow D_2^* e \bar{\nu}_e$  in units of  $\Gamma_0 \tau^2(1)$  for  $\hat{\tau}' = -1.5$ . The notations are the same as in Fig. 3, but the scales are different.

We follow the previous section to obtain expressions for the form factors  $g_i$  in terms of Isgur-Wise functions to order  $\Lambda_{\text{QCD}}/m_Q$ . The fields  $P_v$  and  $P_v^{*\mu}$  that destroy members of the  $s_l^{\pi_l} = \frac{1}{2}^+$  doublet with four-velocity  $v$  are in the  $4 \times 4$  matrix

$$K_v = \frac{1 + \not{v}}{2} [P_v^{*\mu} \gamma_5 \gamma_\mu + P_v]. \quad (3.3)$$

This matrix  $K$  satisfies  $\not{v}K_v = K_v = K_v\not{v}$ . In the infinite mass limit matrix elements of the leading order current operator are [19]

$$\bar{h}_{v'}^{(c)} \Gamma h_v^{(b)} = \zeta(w) \text{Tr} \{ \bar{K}_{v'} \Gamma H_v \} \quad (3.4)$$

Here  $\zeta(w)$  is the leading order Isgur-Wise function ( $\zeta$  is twice the function  $\tau_{1/2}$  of Ref. [19]). Since the  $(D_0^*, D_1^*)$  states are in a different spin multiplet than the ground state,  $g_+(1) = g_{V_1}(1) = 0$  in the infinite mass limit, independent of  $\zeta(1)$ .

The order  $\Lambda_{\text{QCD}}/m_Q$  corrections to the current can be parameterized as

$$\begin{aligned} \bar{h}_{v'}^{(c)} i \overleftarrow{D}_\lambda \Gamma h_v^{(b)} &= \text{Tr} \{ \mathcal{S}_\lambda^{(c)} \bar{K}_{v'} \Gamma H_v \}, \\ \bar{h}_{v'}^{(c)} \Gamma i \overrightarrow{D}_\lambda h_v^{(b)} &= \text{Tr} \{ \mathcal{S}_\lambda^{(b)} \bar{K}_{v'} \Gamma H_v \}. \end{aligned} \quad (3.5)$$

This is the analogue of Eq. (2.8), except that in the present case

$$\mathcal{S}_\lambda^{(Q)} = \zeta_1^{(Q)} v_\lambda + \zeta_2^{(Q)} v'_\lambda + \zeta_3^{(Q)} \gamma_\lambda. \quad (3.6)$$

The functions  $\zeta_i^{(Q)}(w)$  have mass dimension one. The heavy quark equation of motion yield

$$\begin{aligned} w \zeta_1^{(c)} + \zeta_2^{(c)} + \zeta_3^{(c)} &= 0, \\ \zeta_1^{(b)} + w \zeta_2^{(b)} - \zeta_3^{(b)} &= 0. \end{aligned} \quad (3.7)$$

Eq. (2.11) implies  $\mathcal{S}_\lambda^{(c)} + \mathcal{S}_\lambda^{(b)} = (\bar{\Lambda} v_\lambda - \bar{\Lambda}^* v'_\lambda) \zeta$ , which gives three more relations

$$\begin{aligned} \zeta_1^{(c)} + \zeta_1^{(b)} &= \bar{\Lambda} \zeta, \\ \zeta_2^{(c)} + \zeta_2^{(b)} &= -\bar{\Lambda}^* \zeta, \\ \zeta_3^{(c)} + \zeta_3^{(b)} &= 0. \end{aligned} \quad (3.8)$$

These relations express the  $\zeta_j^{(b)}$ 's in terms of the  $\zeta_j^{(c)}$ 's. Combining Eqs. (3.7) with (3.8) yields

$$\begin{aligned} \zeta_2^{(c)} &= -\frac{w\bar{\Lambda}^* - \bar{\Lambda}}{w+1} \zeta - \zeta_1^{(c)}, \\ \zeta_3^{(c)} &= \frac{w\bar{\Lambda}^* - \bar{\Lambda}}{w+1} \zeta - (w-1) \zeta_1^{(c)}. \end{aligned} \quad (3.9)$$

At zero recoil, only  $\zeta_3^{(Q)}$  can give a non-vanishing contribution to the matrix elements of the weak currents in Eq. (3.1). It is determined in terms of  $\bar{\Lambda}^* - \bar{\Lambda}$  and  $\zeta(1)$ , since Eqs. (3.8) and (3.9) imply that

$$\zeta_3^{(c)}(1) = -\zeta_3^{(b)}(1) = \frac{\bar{\Lambda}^* - \bar{\Lambda}}{2} \zeta(1). \quad (3.10)$$

We use Eq. (3.9) to eliminate  $\zeta_2^{(c)}$  and  $\zeta_3^{(c)}$  in favor of  $\zeta_1^{(c)}$  and  $\zeta$ .

There are also order  $\Lambda_{\text{QCD}}/m_Q$  corrections to the effective Lagrangian, given in Eq. (1.4). Time ordered products involving  $O_{\text{kin}}$  can be parameterized as

$$\begin{aligned} i \int d^4x T \left\{ O_{\text{kin},v'}^{(c)}(x) \left[ \bar{h}_{v'}^{(c)} \Gamma h_v^{(b)} \right] (0) \right\} &= \chi_{\text{ke}}^{(c)} \text{Tr} \left\{ \bar{K}_{v'} \Gamma H_v \right\}, \\ i \int d^4x T \left\{ O_{\text{kin},v}^{(b)}(x) \left[ \bar{h}_{v'}^{(c)} \Gamma h_v^{(b)} \right] (0) \right\} &= \chi_{\text{ke}}^{(b)} \text{Tr} \left\{ \bar{K}_{v'} \Gamma H_v \right\}. \end{aligned} \quad (3.11)$$

These corrections do not contribute at zero recoil. The chromomagnetic corrections have the form

$$\begin{aligned} i \int d^4x T \left\{ O_{\text{mag},v'}^{(c)}(x) \left[ \bar{h}_{v'}^{(c)} \Gamma h_v^{(b)} \right] (0) \right\} &= \text{Tr} \left\{ \mathcal{R}_{\alpha\beta}^{(c)} \bar{K}_{v'} i\sigma^{\alpha\beta} \frac{1+\psi'}{2} \Gamma H_v \right\}, \\ i \int d^4x T \left\{ O_{\text{mag},v}^{(b)}(x) \left[ \bar{h}_{v'}^{(c)} \Gamma h_v^{(b)} \right] (0) \right\} &= \text{Tr} \left\{ \mathcal{R}_{\alpha\beta}^{(b)} \bar{K}_{v'} \Gamma \frac{1+\psi'}{2} i\sigma^{\alpha\beta} H_v \right\}, \end{aligned} \quad (3.12)$$

In this case the most general form of  $\mathcal{R}_{\alpha\beta}^{(Q)}$  is

$$\mathcal{R}_{\alpha\beta}^{(c)} = \chi_1^{(c)} \gamma_\alpha \gamma_\beta + \chi_2^{(c)} v_\alpha \gamma_\beta, \quad \mathcal{R}_{\alpha\beta}^{(b)} = \chi_1^{(b)} \gamma_\alpha \gamma_\beta + \chi_2^{(b)} v'_\alpha \gamma_\beta. \quad (3.13)$$

At zero recoil the contribution of  $\chi_2^{(Q)}$  vanish because  $v_\alpha(1+\psi)\sigma^{\alpha\beta}(1+\psi) = 0$ , while that of  $\chi_1^{(Q)}$  vanish because  $(1-\psi)\gamma_\alpha\gamma_\beta(1+\psi) = (1-\psi)(\gamma_\alpha v_\beta - \gamma_\beta v_\alpha)(1+\psi)$ .

Using Eqs. (3.5)–(3.12), it is straightforward to express the form factors  $g_i$  parameterizing  $B \rightarrow D_0^* e \bar{\nu}_e$  and  $B \rightarrow D_1^* e \bar{\nu}_e$  semileptonic decays in terms of Isgur-Wise functions. The order  $\Lambda_{\text{QCD}}/m_b$  Lagrangian corrections arise only in the combination  $\chi_b = \chi_{\text{ke}}^{(b)} + 6\chi_1^{(b)} - 2(w+1)\chi_2^{(b)}$ . Dropping the  $c$  superscript from  $\zeta_1^{(c)}$  and  $\chi_i^{(c)}$ , we obtain

$$\begin{aligned} g_+ &= \varepsilon_c \left[ 2(w-1)\zeta_1 - 3\zeta \frac{w\bar{\Lambda}^* - \bar{\Lambda}}{w+1} \right] - \varepsilon_b \left[ \frac{\bar{\Lambda}^*(2w+1) - \bar{\Lambda}(w+2)}{w+1} \zeta - 2(w-1)\zeta_1 \right], \\ g_- &= \zeta + \varepsilon_c \left[ \chi_{\text{ke}} + 6\chi_1 - 2(w+1)\chi_2 \right] + \varepsilon_b \chi_b. \end{aligned} \quad (3.14)$$

The analogous formulae for  $B \rightarrow D_1^* e \bar{\nu}_e$  are

$$\begin{aligned} g_A &= \zeta + \varepsilon_c \left[ \frac{w\bar{\Lambda}^* - \bar{\Lambda}}{w+1} \zeta + \chi_{\text{ke}} - 2\chi_1 \right] - \varepsilon_b \left[ \frac{\bar{\Lambda}^*(2w+1) - \bar{\Lambda}(w+2)}{w+1} \zeta - 2(w-1)\zeta_1 - \chi_b \right], \\ g_{V_1} &= (w-1)\zeta + \varepsilon_c \left[ (w\bar{\Lambda}^* - \bar{\Lambda})\zeta + (w-1)(\chi_{\text{ke}} - 2\chi_1) \right] \\ &\quad - \varepsilon_b \left\{ [\bar{\Lambda}^*(2w+1) - \bar{\Lambda}(w+2)]\zeta - 2(w^2-1)\zeta_1 - (w-1)\chi_b \right\}, \\ g_{V_2} &= 2\varepsilon_c (\zeta_1 - \chi_2), \\ g_{V_3} &= -\zeta - \varepsilon_c \left[ \frac{w\bar{\Lambda}^* - \bar{\Lambda}}{w+1} \zeta + 2\zeta_1 + \chi_{\text{ke}} - 2\chi_1 + 2\chi_2 \right] \\ &\quad + \varepsilon_b \left[ \frac{\bar{\Lambda}^*(2w+1) - \bar{\Lambda}(w+2)}{w+1} \zeta - 2(w-1)\zeta_1 - \chi_b \right]. \end{aligned} \quad (3.15)$$

These equations show that at zero recoil the leading contributions to  $g_{V_1}$  and  $g_+$  of order  $\Lambda_{\text{QCD}}/m_Q$  are determined in terms of  $\bar{\Lambda}^* - \bar{\Lambda}$  and  $\zeta(1)$ . Explicitly,

$$\begin{aligned} g_+(1) &= -\frac{3}{2} (\varepsilon_c + \varepsilon_b) (\bar{\Lambda}^* - \bar{\Lambda}) \zeta(1), \\ g_{V_1}(1) &= (\varepsilon_c - 3\varepsilon_b) (\bar{\Lambda}^* - \bar{\Lambda}) \zeta(1). \end{aligned} \quad (3.16)$$

For approximation A we shall again expand the double differential decay rates in Eq. (3.2) in powers of  $w - 1$ ,

$$\begin{aligned} \frac{d^2\Gamma_{D_0^*}}{dw d\cos\theta} &= 3\Gamma_0 \zeta^2(1) r_0^{*3} (w^2 - 1)^{3/2} \sin^2\theta \sum_n (w - 1)^n s_0^{(n)}, \\ \frac{d^2\Gamma_{D_1^*}}{dw d\cos\theta} &= 3\Gamma_0 \zeta^2(1) r_1^{*3} \sqrt{w^2 - 1} \sum_n (w - 1)^n \left\{ \sin^2\theta s_1^{(n)} \right. \\ &\quad \left. + (1 - 2r_1^*w + r_1^{*2}) \left[ (1 + \cos^2\theta) t_1^{(n)} - 4\cos\theta \sqrt{w^2 - 1} u_1^{(n)} \right] \right\}. \end{aligned} \quad (3.17)$$

The coefficients for the decay rate into  $D_0^*$  are

$$\begin{aligned} s_0^{(0)} &= (1 - r_0)^{*2} \left[ 1 + 2\varepsilon_c(\hat{\chi}_{\text{ke}} + 6\hat{\chi}_1 - 4\hat{\chi}_2) + 4\varepsilon_b\hat{\chi}_b \right] + 3(\varepsilon_c + \varepsilon_b) (1 - r_0^{*2}) (\bar{\Lambda}^* - \bar{\Lambda}) + \dots, \\ s_0^{(1)} &= 2(1 - r_0^*)^2 \hat{\zeta}' + \dots. \end{aligned} \quad (3.18)$$

For the decay into  $D_1^*$  the coefficients are

$$\begin{aligned} s_1^{(0)} &= (\varepsilon_c - 3\varepsilon_b)^2 (1 - r_1^*)^2 (\bar{\Lambda}^* - \bar{\Lambda})^2 + \dots, \\ s_1^{(1)} &= -2(\varepsilon_c - 3\varepsilon_b) (1 - r_1^{*2}) (\bar{\Lambda}^* - \bar{\Lambda}) + \dots, \\ s_1^{(2)} &= (1 + r_1^*)^2 + \dots, \\ t_1^{(0)} &= (\varepsilon_c - 3\varepsilon_b)^2 (\bar{\Lambda}^* - \bar{\Lambda})^2 + \dots, \\ t_1^{(1)} &= 2 + 4(\varepsilon_c - 3\varepsilon_b) (\bar{\Lambda}^* - \bar{\Lambda}) + 4\varepsilon_c(\hat{\chi}_{\text{ke}} - 2\hat{\chi}_1) + 4\varepsilon_b\hat{\chi}_b + \dots, \\ t_1^{(2)} &= 2(1 + 2\hat{\zeta}') + \dots, \\ u_1^{(0)} &= (\varepsilon_c - 3\varepsilon_b) (\bar{\Lambda}^* - \bar{\Lambda}) + \dots, \\ u_1^{(1)} &= 1 + \dots. \end{aligned} \quad (3.19)$$

Note that at zero recoil and at order  $w - 1$  the contributions to  $D_1^*$  decay proportional to  $\bar{\Lambda}^* - \bar{\Lambda}$  depend on the anomalously small combination  $\varepsilon_c - 3\varepsilon_b \sim 0.05\text{GeV}^{-1}$ . Thus  $\Lambda_{\text{QCD}}/m_Q$  corrections enhance  $B \rightarrow D_1^*$  by a much smaller amount than they enhance  $B \rightarrow D_1$  decay. On the other hand, the  $B \rightarrow D_0^*$  decay rate receives a large enhancement from  $\Lambda_{\text{QCD}}/m_Q$  corrections, similar to  $B \rightarrow D_1$ .

In approximation A,  $B \rightarrow D_1^*$  is treated the same way as  $B \rightarrow D_1$  in Sec. II.  $B \rightarrow D_0^*$  is treated as  $B \rightarrow D_2^*$  in Sec. II, since these rates contain an additional factor of  $w^2 - 1$ . Approximation B is also very similar to that in Sec. II, except that in the present case there is only one unknown  $\Lambda_{\text{QCD}}/m_Q$  Isgur-Wise function,  $\zeta_1$  (once time ordered products involving the chromomagnetic operator are neglected, and the matrix elements of the time ordered

products involving the kinetic energy operator are absorbed into the  $m_Q \rightarrow \infty$  Isgur-Wise function,  $\zeta$ ). In approximation B<sub>1</sub> we set  $\zeta_1 = 0$  in Eqs. (3.14) and (3.15). This is identical to saturating the first relation in Eq. (3.8) by  $\zeta_1^{(b)}$ , i.e., setting  $\zeta_1^{(b)} = \bar{\Lambda} \zeta$ . In approximation B<sub>2</sub> we set  $\zeta_1 = \bar{\Lambda} \zeta$  in Eqs. (3.14) and (3.15), which is identical to setting  $\zeta_1^{(b)} = 0$ . To the extent the first relation in Eq. (3.8) can be taken as a hint to the sign of  $\zeta_1$ , the difference between approximations B<sub>1</sub> and B<sub>2</sub> gives a crude estimate of the uncertainty related to the unknown  $\Lambda_{\text{QCD}}/m_Q$  corrections.

As in the previous section, the expression for the decay rate in terms of form factors in Eq. (3.2) implies that  $s_1^{(0)}/t_1^{(0)} = (1 - r_1^*)^2$  to all orders in the  $\Lambda_{\text{QCD}}/m_Q$  expansion. Thus the ratio of helicity zero and helicity one  $B \rightarrow D_1^*$  decay rates at zero recoil is  $\lim_{w \rightarrow 1} \left[ (d\Gamma_{D_1^*}^{(\lambda=0)}/dw) / (d\Gamma_{D_1^*}^{(|\lambda|=1)}/dw) \right] = 1/2$ .

### A. Predictions

A model independent prediction similar to that in Sec. II can be made for the slope parameter of semileptonic  $B$  decay into the helicity zero  $D_1^*$ . We write the semileptonic decay rate into the helicity zero  $D_1^*$  as

$$\frac{d\Gamma_{D_1^*}^{(\lambda=0)}}{dw} = 4\Gamma_0 r_1^{*3} (1 - r_1^*)^2 \sqrt{w^2 - 1} \zeta^2(1) (\varepsilon_c - 3\varepsilon_b)^2 (\bar{\Lambda}^* - \bar{\Lambda})^2 \left[ 1 - \rho_{D_1^*}^2 (w - 1) + \dots \right]. \quad (3.20)$$

The relationship between  $s_1^{(0)}$  and  $s_1^{(1)}$  implies that the slope parameter  $\rho_{D_1^*}^2$  for helicity zero  $D_1^*$  is

$$\rho_{D_1^*}^2 = \frac{1 + r_1^*}{1 - r_1^*} \frac{2}{(\varepsilon_c - 3\varepsilon_b) (\bar{\Lambda}^* - \bar{\Lambda})} + \mathcal{O}(1). \quad (3.21)$$

As in Sec. II, this slope parameter is of order  $m_Q/\Lambda_{\text{QCD}}$ . It would be very hard experimentally to test this model independent prediction, since the  $D_1^*$  is expected to be of order 100 MeV broad, and also because  $\varepsilon_c - 3\varepsilon_b$  is so small.

Predictions for the  $B \rightarrow D_0^* e \bar{\nu}_e$  and  $B \rightarrow D_1^* e \bar{\nu}_e$  rates are shown in the first two columns of Table IV, normalized to  $\zeta^2(1)$  times the measured  $B \rightarrow D_1 e \bar{\nu}_e$  rate. These results are obtained using  $\hat{\zeta}' = -1$ , and  $\bar{\Lambda}^* - \bar{\Lambda} \simeq 0.35$  GeV corresponding to  $1 < w < 1.33$ . This value of  $\bar{\Lambda}^* - \bar{\Lambda}$  has at least a 50 MeV uncertainty at present, as it follows from model predictions for the masses of the  $s_\ell^{\pi\ell} = \frac{1}{2}^+$  charmed mesons,  $\bar{m}_D^* \simeq 2.40$  GeV [26], and from the fact that  $\lambda_1^* = \lambda_1'$  in nonrelativistic quark models with spin-orbit independent potentials. Although the  $D_1^*$  state is expected to be somewhat heavier than the  $D_0^*$ , we use the kinematic range  $1 < w < 1.33$  for both decays. The results in the first two columns of Table IV are quite sensitive to the value of  $\hat{\zeta}'$  and  $\hat{\zeta}_1$ . In approximation B<sub>1</sub>, for example,  $\mathcal{B}(B \rightarrow D_0^* e \bar{\nu}_e)/[\zeta^2(1) \times 0.006]$  changes from 1.92 at  $\hat{\zeta}' = 0$  to 0.54 at  $\hat{\zeta}' = -2$ . In the same range of  $\hat{\zeta}'$ ,  $\mathcal{B}(B \rightarrow D_1^* e \bar{\nu}_e)/[\zeta^2(1) \times 0.006]$  changes from 0.72 to 0.24. The effect of  $\hat{\zeta}_1$  is also important; in the range  $-0.75$  GeV  $< \hat{\zeta}_1 < 0.75$  GeV, the  $D_0^*$  and  $D_1^*$  branching ratios change from 1.68 to 0.66 and 0.30 to 0.63, respectively. Therefore, even if  $\zeta$  were known



Approximation	$\frac{\mathcal{B}(B \rightarrow D_0^* e \bar{\nu}_e)}{\zeta^2(1) \times 0.006}$	$\frac{\mathcal{B}(B \rightarrow D_1^* e \bar{\nu}_e)}{\zeta^2(1) \times 0.006}$	$\Gamma_{D_0^*+D_1^*}/\Gamma_{D_1}$
A <sub>∞</sub>	0.30	0.66	1.07
B <sub>∞</sub>	0.33	0.46	1.61
A	1.03	0.65	0.80
B <sub>1</sub>	1.11	0.44	1.03
B <sub>2</sub>	0.85	0.53	1.05

TABLE IV. The first two columns show semileptonic  $B$  branching ratios into  $D_0^*$  and  $D_1^*$  normalized to  $\zeta^2(1)$  times the measured branching ratio  $\mathcal{B}(B \rightarrow D_1 e \bar{\nu}_e) = 0.6\%$ , assuming  $\hat{\zeta}' = \zeta'(1)/\zeta(1) = -1$ . The sum of  $D_0^* + D_1^*$  rates relative to  $B \rightarrow D_1$  is in the third column, using the nonrelativistic constituent quark model prediction in Eq. (3.22) and  $\hat{\tau}' = -1.5$ .

from models or lattice calculations, there would still be a factor of two uncertainty in the theoretical predictions for the semileptonic  $B \rightarrow D_0^*$  and  $D_1^*$  rates; but the uncertainty in the sum of these two rates is smaller.

To obtain even a crude absolute prediction for the  $B \rightarrow D_1^*, D_0^*$  rates, a relation between the  $s_\ell^{\pi_\ell} = \frac{1}{2}^+$  and  $\frac{3}{2}^+$  Isgur-Wise functions is needed. In any nonrelativistic constituent quark model with spin-orbit independent potential,  $\zeta$  and  $\tau$  are related by [24,19]

$$\zeta(w) = \frac{w+1}{\sqrt{3}} \tau(w), \quad (3.22)$$

since both of these spin symmetry doublets correspond to  $L = 1$  orbital excitations. This implies

$$\zeta(1) = \frac{2}{\sqrt{3}} \tau(1), \quad \hat{\zeta}' = \frac{1}{2} + \hat{\tau}'. \quad (3.23)$$

In the same approximation,  $\hat{\eta}_{\text{ke}} = \hat{\chi}_{\text{ke}}$ .<sup>7</sup>

Predictions for the  $B$  semileptonic decay rate into the states in the  $s_\ell^{\pi_\ell} = \frac{1}{2}^+$  doublet that follow from Eq. (3.23) are shown in the last column of Table IV. (For this quantity, approximations  $B_i$  ( $i = 1, 2$ ) contain a somewhat ad hoc input of combining the  $B_i$  prediction in Sec. II with the  $B_i$  prediction for  $B \rightarrow D_0^*, D_1^*$ .) For  $\hat{\tau}' = -1.5$ , the  $\frac{1}{2}^+$  doublet contributes about  $1.0 \times \mathcal{B}(B \rightarrow D_1 e \bar{\nu}_e) \sim 0.6\%$  to the total  $B$  decay rate. Varying  $\tau_{1,2}$  and  $\zeta_1$  in approximation B results in the range  $(0.6 - 1.7) \times \mathcal{B}(B \rightarrow D_1 e \bar{\nu}_e)$  for the sum of the  $D_0^*$  and  $D_1^*$  rates. This combined with our results for  $R = \Gamma_{D_2^*}/\Gamma_{D_1}$  in Sec. II is consistent with the ALEPH measurement [15] of the branching ratio for the sum of all semileptonic decays containing a  $D^{(*)} \pi$  in the final state to be  $(2.26 \pm 0.44)\%$ .

The semileptonic decay rate into  $D$  and  $D^*$  is about 6.6% of the total  $B$  decay rate [9]. Our results then suggest that the six lightest charmed mesons contribute about 8.2% of the  $B$  decay rate. Therefore, semileptonic decays into higher excited states and non-resonant

<sup>7</sup>A relation between  $\tau_{1,2}$  and  $\zeta_1$  may also hold in this model.

multi-body channels should be at least 2% of the  $B$  decay rate, and probably around 3% if the semileptonic  $B$  branching ratio is closer to the LEP result of about 11.5%. Such a sizable contribution to the semileptonic rate from higher mass excited charmed mesons and non-resonant modes would soften the lepton spectrum, and may make the agreement with data on the inclusive lepton spectrum worse. Of course, the decay rates to the broad  $\frac{1}{2}^+$  states would change substantially if the nonrelativistic quark model prediction in Eq. (3.22) is wrong. Semileptonic  $B$  decay rate to the six lightest charmed mesons could add up to close to 10% if  $\zeta$  were enhanced by a factor of two compared to the prediction of Eq. (3.22). However, model calculations [25] seem to obtain a suppression rather than an enhancement of  $\zeta$  compared to Eq. (3.22). Thus, taking the measurements for the  $B \rightarrow D, D^*,$  and  $D_1$  semileptonic branching ratios on face value, a decomposition of the semileptonic rate as a sum of exclusive channels seems problematic both in light of our results and the above ALEPH measurement for the sum of all semileptonic decays containing a  $D^{(*)} \pi$  in the final state.

#### IV. OTHER EXCITED CHARMED MESONS AT ZERO RECOIL

In the previous two sections matrix elements of the weak vector current and axial-vector current between a  $B$  meson and an excited charmed mesons with  $s_\ell^{\pi_\ell} = \frac{3}{2}^+$  and  $\frac{1}{2}^+$  quantum numbers were considered. Here we consider such matrix elements at zero recoil for excited charmed mesons with other  $s_\ell^{\pi_\ell}$  quantum numbers. Only charmed mesons with spin zero or spin one can contribute at this kinematic point. The polarization tensor of a spin  $n$  state is rank  $n$ , traceless and symmetric in its indices, and vanishes if it is contracted with the 4-velocity of the state. For matrix elements of the axial-vector or vector current, at least  $n - 1$  indices of the charmed meson polarization tensor are contracted with  $v^\mu$ , the four velocity of the  $B$  meson. Consequently, for  $n > 1$  these matrix elements vanish at zero recoil, where  $v = v'$ . In this section we work in the rest frame,  $v = v' = (1, \vec{0})$ , and four-velocity labels on the fields and states are suppressed.

For spin zero and spin one excited charmed mesons, the possible spin parities for the light degrees of freedom are  $s_\ell^{\pi_\ell} = \frac{1}{2}^+, \frac{3}{2}^+$ , which we have already considered in the previous sections, and  $s_\ell^{\pi_\ell} = \frac{1}{2}^-, \frac{3}{2}^-$ . In the nonrelativistic constituent quark model, the  $\frac{1}{2}^-$  states are interpreted as radial excitations of the ground state ( $D, D^*$ ) doublet and the  $\frac{3}{2}^-$  states are  $L = 2$  orbital excitations. In the quark model, these states are typically expected to be broad. The mass of the lightest  $s_l^{\pi_l} = \frac{3}{2}^-$  doublet is expected around 2.8 GeV, while the lightest excited states with  $s_l^{\pi_l} = \frac{1}{2}^-$  are expected around 2.6 GeV [26].<sup>8</sup> ( $B$  decays into radial excitations of the  $s_l^{\pi_l} \neq \frac{1}{2}^-$  states have similar properties as the decay into the lightest state with the same quantum numbers.)

---

<sup>8</sup>The lightest  $\frac{1}{2}^-$  states may be narrow since decays to the  $s_\ell^{\pi_\ell} = \frac{1}{2}^-$  and  $\frac{3}{2}^-$  multiplets are suppressed by the available phase space, and decays to  $D^{(*)} \pi$  in an  $S$ -wave are forbidden by parity.

In the  $m_Q \rightarrow \infty$  limit, the zero recoil matrix elements vanish by heavy quark symmetry. For the excited  $s_\ell^{\pi\ell} = \frac{1}{2}^-$  states, the  $m_Q \rightarrow \infty$  Isgur-Wise functions vanish at zero recoil due to the orthogonality of the states. The matrix elements for the  $s_\ell^{\pi\ell} \neq \frac{1}{2}^-$  states vanish at zero recoil due to spin symmetry alone, and therefore the corresponding  $m_Q \rightarrow \infty$  Isgur-Wise functions need not vanish at zero recoil.

Using the same methods as in Sections II and III, it is straightforward to show that  $\Lambda_{\text{QCD}}/m_Q$  corrections to the current do not contribute at zero recoil. For the  $s_\ell^{\pi\ell} = \frac{1}{2}^-$  states, this follows from the heavy quark equation of motion. For the  $s_\ell^{\pi\ell} = \frac{3}{2}^-$  states, the  $\Lambda_{\text{QCD}}/m_Q$  corrections to the current can be parameterized similar to Eqs. (2.8) and (2.9). In this case the analogue of  $F_v^\mu$  in Eq. (2.5) satisfies  $\psi F_v^\mu = F_v^\mu \psi = F_v^\mu \psi$ . Recall that the  $\tau_4^{(Q)} g_{\sigma\lambda}$  in Eq. (2.9) was the only term whose contribution at zero recoil did not vanish due to the  $v_\mu F_v^\mu = 0$  property of the Rarita-Schwinger spinors. Here, the analogous term is placed between  $1 - \psi$  and  $1 + \psi'$ , and therefore also disappears at  $v = v'$ .

It remains to consider the  $\Lambda_{\text{QCD}}/m_Q$  contributions to the  $\frac{1}{2}^-$  and  $\frac{3}{2}^-$  matrix elements coming from corrections to the Lagrangian in Eq. (1.4). These are written as time ordered products of  $O_{\text{kin}}^{(Q)}(x)$  and  $O_{\text{mag}}^{(Q)}(x)$  with the leading order  $m_Q \rightarrow \infty$  currents (e.g., Eq (2.16)). At zero recoil it is useful to insert a complete set of states between these operators. Since the zero recoil weak currents are charge densities of heavy quark spin-flavor symmetry, only one state from this sum contributes. For the  $s_\ell^{\pi\ell} = \frac{1}{2}^-$  multiplet this procedure gives

$$\frac{\langle D^{*(n)}(\varepsilon) | \vec{A} | B \rangle}{\sqrt{m_{D^{*(n)}} m_B}} = \frac{-\vec{\varepsilon}}{(\bar{\Lambda}^{(n)} - \bar{\Lambda})} \left\{ \left( \frac{1}{2m_c} + \frac{3}{2m_b} \right) \frac{\langle D^{*(n)}(\varepsilon) | O_{\text{mag}}^{(c)}(0) | D^*(\varepsilon) \rangle}{\sqrt{m_{D^{*(n)}} m_{D^*}}} \right. \\ \left. + \left( \frac{1}{2m_c} - \frac{1}{2m_b} \right) \frac{\langle D^{*(n)}(\varepsilon) | O_{\text{kin}}^{(c)}(0) | D^*(\varepsilon) \rangle}{\sqrt{m_{D^{*(n)}} m_{D^*}}} \right\}. \quad (4.1)$$

and

$$\frac{\langle D^{(n)} | V^0 | B \rangle}{\sqrt{m_{D^{(n)}} m_B}} = \frac{1}{(\bar{\Lambda}^{(n)} - \bar{\Lambda})} \left( -\frac{1}{2m_c} + \frac{1}{2m_b} \right) \frac{\langle D^{(n)} | O_{\text{mag}}^{(c)}(0) + O_{\text{kin}}^{(c)}(0) | D \rangle}{\sqrt{m_{D^{(n)}} m_D}}. \quad (4.2)$$

Here we have denoted spin zero and spin one members of the excited  $s_\ell^{\pi\ell} = \frac{1}{2}^-$  multiplet by  $D^{(n)}$  and  $D^{*(n)}$  respectively, and the analogues of  $\bar{\Lambda}$  by  $\bar{\Lambda}^{(n)}$ . Heavy quark spin-flavor symmetry was used to write the effects of  $O_{\text{kin}}^{(b)}$  and  $O_{\text{mag}}^{(b)}$  in terms of matrix elements of  $O_{\text{kin}}^{(c)}$  and  $O_{\text{mag}}^{(c)}$ . This neglects the weak logarithmic dependence on the heavy quark mass in the matrix elements of  $O_{\text{mag}}$ . For the spin one member of the  $s_\ell^{\pi\ell} = \frac{3}{2}^-$  multiplet, which we denote by  $D_1^{**}$ ,

$$\frac{\langle D_1^{**}(\varepsilon) | \vec{A} | B \rangle}{\sqrt{m_{D_1^{**}} m_B}} = \frac{-\vec{\varepsilon}}{(\bar{\Lambda}^{**} - \bar{\Lambda})} \left( \frac{1}{2m_c} \right) \frac{\langle D_1^{**}(\varepsilon) | O_{\text{mag}}^{(c)}(0) | D^*(\varepsilon) \rangle}{\sqrt{m_{D_1^{**}} m_D}}. \quad (4.3)$$

For the  $s_\ell^{\pi\ell} = \frac{1}{2}^-$  and  $\frac{3}{2}^-$  excited charmed mesons, the correction to the Lagrangian,  $\delta\mathcal{L}$  in Eq. (1.4), gives rise to an order  $\Lambda_{\text{QCD}}/m_c$  contribution to the matrix elements of the weak currents at zero recoil. Formulae similar to those in Eqs. (4.1)–(4.3) hold in the  $s_\ell^{\pi\ell} = \frac{1}{2}^+$ ,  $\frac{3}{2}^+$  cases, but the corresponding matrix elements vanish due to the parity invariance of the strong interaction.

Approximation	$\frac{\mathcal{B}(B \rightarrow D_1 \pi)}{\mathcal{B}(B \rightarrow D_1 e \bar{\nu}_e)}$	$\frac{\mathcal{B}(B \rightarrow D_2^* \pi)}{\mathcal{B}(B \rightarrow D_1 \pi)}$
A <sub>∞</sub>	0.39	0.36
B <sub>∞</sub>	0.26	1.00
A	0.29	0.21
B <sub>1</sub>	0.19	0.41
B <sub>2</sub>	0.20	0.56

TABLE V. Predictions for the ratios of branching ratios,  $\mathcal{B}(B \rightarrow D_1 \pi)/\mathcal{B}(B \rightarrow D_1 e \bar{\nu}_e)$  and  $\mathcal{B}(B \rightarrow D_2^* \pi)/\mathcal{B}(B \rightarrow D_1 \pi)$ , using factorization and assuming  $\hat{\tau}' = \tau'(1)/\tau(1) = -1.5$ .

## V. APPLICATIONS

### A. Factorization

Factorization should be a good approximation for  $B$  decay into charmed mesons and a charged pion. Contributions that violate factorization are suppressed by  $\Lambda_{\text{QCD}}$  divided by the energy of the pion in the  $B$  rest frame [27] or by  $\alpha_s(m_Q)$ . Furthermore for these decays, factorization also holds in the limit of large number of colors. Neglecting the pion mass, the two-body decay rate,  $\Gamma_\pi$ , is related to the differential decay rate  $d\Gamma_{\text{sl}}/dw$  at maximal recoil for the analogous semileptonic decay (with the  $\pi$  replaced by the  $e \bar{\nu}_e$  pair). This relation is independent of the identity of the charmed meson in the final state,

$$\Gamma_\pi = \frac{3\pi^2 |V_{ud}|^2 C^2 f_\pi^2}{m_B^2 r} \times \left( \frac{d\Gamma_{\text{sl}}}{dw} \right)_{w_{\text{max}}} . \quad (5.1)$$

Here  $r$  is the mass of the charmed meson divided by  $m_B$ ,  $w_{\text{max}} = (1 + r^2)/(2r)$ , and  $f_\pi \simeq 132 \text{ MeV}$  is the pion decay constant.  $C$  is a combination of Wilson coefficients of four-quark operators, and numerically  $C |V_{ud}|$  is very close to unity.

These nonleptonic decay rates can therefore be predicted from a measurement of  $d\Gamma_{\text{sl}}/dw$  at maximal recoil. The semileptonic decay rate near maximal recoil is only measured for  $B \rightarrow D^{(*)} e \bar{\nu}_e$  at present. The measured  $B \rightarrow D^{(*)} \pi$  rate is consistent with Eq. (5.1) at the level of the 10% experimental uncertainties. In the absence of a measurement of the  $B \rightarrow (D_1, D_2^*) e \bar{\nu}_e$  differential decay rates, we can use our results for the shape of  $d\Gamma_{\text{sl}}/dw$  to predict the  $B \rightarrow D_1 \pi$  and  $B \rightarrow D_2^* \pi$  decay rates. These predictions depend on the semileptonic differential decay rates at  $w_{\text{max}}$ , where we are the least confident that  $\Lambda_{\text{QCD}}/m_Q$  terms involving  $\bar{\Lambda}$  and  $\bar{\Lambda}'$  are the most important. With this caveat in mind, we find the results shown in Table V.

At present there are only crude measurements of the  $\mathcal{B}(B \rightarrow D_1 \pi)$  and  $\mathcal{B}(B \rightarrow D_2^* \pi)$  branching ratios. Assuming  $\mathcal{B}(D_1(2420)^0 \rightarrow D^{*+} \pi^-) = 2/3$  and  $\mathcal{B}(D_2^*(2460)^0 \rightarrow D^{*+} \pi^-) = 0.2$ , the measured rates are [28]

$$\begin{aligned} \mathcal{B}(B^- \rightarrow D_1(2420)^0 \pi^-) &= (1.17 \pm 0.29) \times 10^{-3}, \\ \mathcal{B}(B^- \rightarrow D_2^*(2460)^0 \pi^-) &= (2.1 \pm 0.9) \times 10^{-3}. \end{aligned} \quad (5.2)$$

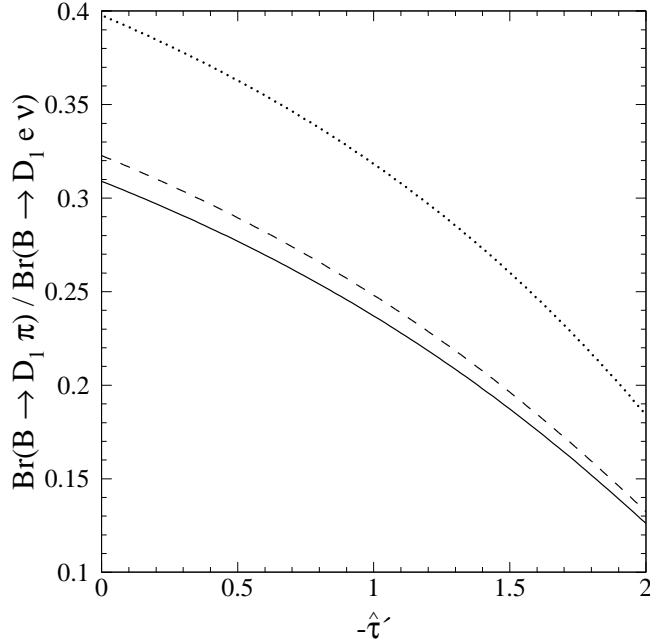


FIG. 5. Factorization prediction for  $\mathcal{B}(B \rightarrow D_1 \pi)/\mathcal{B}(B \rightarrow D_1 e \bar{\nu}_e)$  as a function of  $\hat{\tau}' = \tau'(1)/\tau(1)$ . The dotted curve shows the  $m_Q \rightarrow \infty$  limit ( $B_\infty$ ), solid curve is approximation  $B_1$ , dashed curve is  $B_2$ .

A reduction of the experimental uncertainty in  $\mathcal{B}(B \rightarrow D_2^* \pi)$  is needed to test the prediction in the second column of Table V.

The prediction for  $\mathcal{B}(B \rightarrow D_1 \pi)/\mathcal{B}(B \rightarrow D_1 e \bar{\nu}_e)$  in approximation B is fairly independent of  $\tau_{1,2}$ , but more sensitive to  $\hat{\tau}'$ . The latter dependence is plotted in Fig. 5 for  $0 > \hat{\tau}' > -2$ . Not absorbing  $\eta_{ke}$  into  $\tau$  results in the following weak dependence:  $\mathcal{B}(B \rightarrow D_1 \pi)/\mathcal{B}(B \rightarrow D_1 e \bar{\nu}_e) \propto 1 + 0.27 \varepsilon_c \hat{\eta}_{ke} + \dots$ . Assuming that factorization works at the 10% level, a precise measurement of the  $\mathcal{B}(B \rightarrow D_1 \pi)$  rate may provide a determination of  $\hat{\tau}'$ . The present experimental data,  $\mathcal{B}(B \rightarrow D_1 \pi)/\mathcal{B}(B \rightarrow D_1 e \bar{\nu}_e) \simeq 0.2$ , does in fact support  $\hat{\tau}' \sim -1.5$ , which we took as the “central value” in this paper, motivated by model calculations.

The prediction for  $\mathcal{B}(B \rightarrow D_2^* \pi)/\mathcal{B}(B \rightarrow D_1 \pi)$ , on the other hand, only weakly depends on  $\hat{\tau}'$ , but it is more sensitive to  $\tau_{1,2}$ . Varying  $\tau_{1,2}$  in the range  $-0.75 \text{ GeV} < \hat{\tau}_{1,2} < 0.75 \text{ GeV}$ , we can accommodate almost any value of  $\mathcal{B}(B \rightarrow D_2^* \pi)/\mathcal{B}(B \rightarrow D_1 \pi)$  between 0 and 1.5. This quantity depends more sensitively on  $\tau_1$  than on  $\tau_2$ . In Fig. 6 we plot  $\mathcal{B}(B \rightarrow D_2^* \pi)/\mathcal{B}(B \rightarrow D_1 \pi)$  in approximation B as a function of  $\hat{\tau}_1$  setting  $\hat{\tau}_2 = 0$  (solid curve), and as a function of  $\hat{\tau}_2$  setting  $\hat{\tau}_1 = 0$  (dashed curve). Not absorbing  $\eta_{ke}$  into  $\tau$  results in the following dependence:  $\mathcal{B}(B \rightarrow D_2^* \pi)/\mathcal{B}(B \rightarrow D_1 \pi) \propto 1 + 0.75 \varepsilon_c \hat{\eta}_{ke} + \dots$ . This ratio and  $R$  depend on  $\hat{\eta}_{ke}$  and  $\hat{\tau}_1$ . In the future experimental data on these ratios may lead to a determination of  $\hat{\eta}_{ke}$  and  $\hat{\tau}_1$ .

If the experimental central value on  $\mathcal{B}(B \rightarrow D_2^* \pi)$  does not decrease compared to Eq. (5.2), then it would suggest a huge value for  $\hat{\tau}_1$ , leading to a violation of the ALEPH bound on  $R$  (see Fig. 1). The approximation B results in Tables II and V can be combined to give  $\mathcal{B}(B \rightarrow D_2^* \pi)/\mathcal{B}(B \rightarrow D_2^* e \bar{\nu}_e) = 0.15$ . Varying  $\hat{\tau}_i$ ,  $\hat{\eta}_{ke}$  and  $\hat{\tau}'$  does not bring

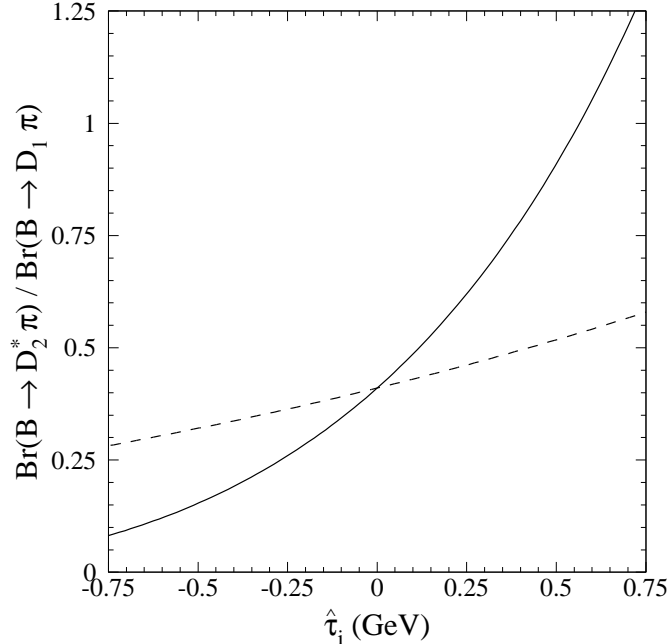


FIG. 6. Factorization prediction for  $\mathcal{B}(B \rightarrow D_2^* \pi) / \mathcal{B}(B \rightarrow D_1 \pi)$  as a function of  $\hat{\tau}_1 (= \tau_1 / \tau)$  for  $\hat{\tau}_2 = 0$  (solid curve), and as a function of  $\hat{\tau}_2$  for  $\hat{\tau}_1 = 0$  (dashed curve).

this quantity close to the current experimental limit. Therefore, if the branching ratio for  $B \rightarrow D_2^* e \bar{\nu}_e$  is below the ALEPH bound, then  $\mathcal{B}(B \rightarrow D_2^* \pi)$  should be smaller than the central value in Eq. (5.2).

## B. Sum Rules

Our results are important for sum rules that relate inclusive  $B \rightarrow X_c e \bar{\nu}_e$  decays to the sum of exclusive channels. The Bjorken sum rule bounds the slope of the  $B \rightarrow D^{(*)} e \bar{\nu}_e$  Isgur-Wise function, defined by the expansion  $\xi(w) = 1 - \rho^2 (w - 1) + \dots$ . Knowing  $\rho^2$  would reduce the uncertainty in the determination of  $|V_{cb}|$  from the extrapolation of the  $B \rightarrow D^{(*)} e \bar{\nu}_e$  spectrum to zero recoil. The Bjorken sum rule [29,19] is

$$\rho^2 = \frac{1}{4} + \sum_m \frac{|\zeta^{(m)}(1)|^2}{4} + 2 \sum_p \frac{|\tau^{(p)}(1)|^2}{3} + \dots \quad (5.3)$$

Throughout this section the ellipses denote contributions from non-resonant channels.  $\zeta^{(m)}$  and  $\tau^{(p)}$  are the Isgur-Wise functions for the excited  $s_\ell^{\pi_\ell} = \frac{1}{2}^+$  and  $\frac{3}{2}^+$  states, respectively (for  $m = p = 0$  these are the orbitally excited states discussed in Sec. II and III, and  $m, p \geq 1$  are radial excitations of these).<sup>9</sup> Since all terms in the sums, as well as the contributions replaced by ellipses, are non-negative, a lower bound on  $\rho^2$  can be obtained by keeping only

<sup>9</sup>In Ref. [19]  $|\zeta^{(m)}(1)|^2/4$  was denoted by  $|\tau_{1/2}^{(m)}(1)|^2$ , and  $|\tau^{(p)}(1)|^2/3$  was denoted by  $|\tau_{3/2}^{(p)}(1)|^2$ .

the first few terms on the right-hand-side of Eq. (5.3). Using Eqs. (2.31) and (3.22), we find that the contribution of the lowest lying  $s_\ell^{\pi_\ell} = \frac{1}{2}^+$  and  $\frac{3}{2}^+$  states implies the bound

$$\rho^2 > \frac{1}{4} + \frac{|\zeta(1)|^2}{4} + 2 \frac{|\tau(1)|^2}{3} \simeq 0.75. \quad (5.4)$$

The contribution of the  $\frac{1}{2}^+$  states through  $\zeta(1)$  to this bound, which relies on the quark model result in Eq. (3.22), is only 0.17.

An upper bound on  $\rho^2$  follows from an upper bound on the excited states contribution to the right-hand-side of Eq. (5.3). This sum rule was first derived by Voloshin [30]

$$\frac{1}{2} \bar{\Lambda} = \sum_m (\bar{\Lambda}^{*(m)} - \bar{\Lambda}) \frac{|\zeta^{(m)}(1)|^2}{4} + 2 \sum_p (\bar{\Lambda}'^{(p)} - \bar{\Lambda}) \frac{|\tau^{(p)}(1)|^2}{3} + \dots \quad (5.5)$$

Here  $\bar{\Lambda}^{*(m)}$  and  $\bar{\Lambda}'^{(p)}$  are the analogues of  $\bar{\Lambda}^*$  and  $\bar{\Lambda}'$  for the excited  $s_\ell^{\pi_\ell} = \frac{1}{2}^+$  and  $\frac{3}{2}^+$  states, respectively. Eq. (5.5) combined with Eq. (5.3) implies that  $\rho^2 < 1/4 + \bar{\Lambda}/(2\varepsilon_1)$ , where  $\varepsilon_1$  is the excitation energy of the lightest excited charmed meson state. However, knowing  $\zeta(1)$  and  $\tau(1)$  does not strengthen this bound on  $\rho^2$  significantly. On the other hand, Eq. (5.5) implies the bound  $\bar{\Lambda} > 0.38 \text{ GeV}$  (neglecting perturbative QCD corrections). The model dependent contribution of the  $\frac{1}{2}^+$  states to this bound is only 0.12 GeV; while the bound  $\bar{\Lambda} > 0.26 \text{ GeV}$  from only the  $\frac{3}{2}^+$  states is fairly model independent.

A class of zero recoil sum rules were considered in Ref. [31]. The axial sum rule, which bounds the  $B \rightarrow D^*$  form factor (that is used to determine  $|V_{cb}|$ ) only receives contributions from  $s_\ell^{\pi_\ell} = \frac{1}{2}^-$  and  $\frac{3}{2}^-$  states, which were discussed in Sec. IV. It has the form

$$|F_{B \rightarrow D^*}(1)|^2 + \sum_{X_c} \frac{|\langle X_c(\varepsilon) | \vec{A} | B \rangle|^2}{4m_{X_c} m_B} = \eta_A^2 - \frac{\lambda_2}{m_c^2} + \frac{\lambda_1 + 3\lambda_2}{4} \left( \frac{1}{m_c^2} + \frac{1}{m_b^2} + \frac{2}{3m_c m_b} \right), \quad (5.6)$$

where  $\eta_A$  is the perturbative matching coefficient of the full QCD axial-vector current onto the HQET current,  $X_c$  denotes spin one states (continuum or resonant) with  $s_\ell^{\pi_\ell} = \frac{1}{2}^-$  and  $\frac{3}{2}^-$ , and  $F_{B \rightarrow D^*}(1)$  is defined by

$$\frac{\langle D^*(\varepsilon) | \vec{A} | B \rangle}{2\sqrt{m_{D^*} m_B}} = F_{B \rightarrow D^*}(1) \vec{\varepsilon}. \quad (5.7)$$

Neglecting the contributions of the excited states  $X_c$  to the left-hand-side, gives an upper bound on  $|F_{B \rightarrow D^*}(1)|^2$ . Using the nonrelativistic constituent quark model, we estimate using Eq. (4.1) that the contribution of the first radial excitation of the  $D^*$  to the sum over  $X_c$  in Eq. (5.6) is about 0.1. For this estimate we took  $\bar{\Lambda}^{(1)} - \bar{\Lambda} = 450 \text{ MeV}$ ,  $O_{\text{mag}}^{(c)} = C \delta^3(r) \vec{s}_c \cdot \vec{s}_{\bar{q}}$  (fixing the constant  $C$  by the measured  $D^* - D$  mass splitting),  $O_{\text{kin}}^{(c)} = \vec{\nabla}^2$ , and used the harmonic oscillator quark model wave functions of Ref. [22]. A 0.1 correction would significantly strengthen the upper bound on  $F_{B \rightarrow D^*}(1)$  and have important consequences for the extraction of the magnitude of  $V_{cb}$  from exclusive  $B \rightarrow D^* e \bar{\nu}_e$  decay. Note that  $s_\ell^{\pi_\ell} = \frac{3}{2}^-$  states do not contribute to the zero recoil axial sum rule in the quark model, because their spatial wave functions vanish at the origin.

The  $J^P = 1^+$  members of the  $s_{\ell}^{\pi\ell} = \frac{1}{2}^+$  and  $s_{\ell}^{\pi\ell} = \frac{3}{2}^+$  doublets contribute to the vector sum rule, which is used to bound  $\lambda_1$ . This sum rule reads [31,2]

$$\begin{aligned} & \frac{(m_b - 3m_c)^2}{4m_b^2 m_c^2} \sum_m (\bar{\Lambda}^{*(m)} - \bar{\Lambda})^2 \frac{|\zeta^{(m)}(1)|^2}{4} + \frac{2}{m_c^2} \sum_p (\bar{\Lambda}'^{(p)} - \bar{\Lambda})^2 \frac{|\tau^{(p)}(1)|^2}{3} + \dots \\ & = \frac{\lambda_2}{m_c^2} - \frac{\lambda_1 + 3\lambda_2}{4} \left( \frac{1}{m_c^2} + \frac{1}{m_b^2} - \frac{2}{3m_c m_b} \right). \end{aligned} \quad (5.8)$$

This relation can be simplified by setting  $m_b/m_c$  to different values. Taking  $m_b = m_c$  yields

$$\lambda_1 = -3 \sum_m (\bar{\Lambda}^{*(m)} - \bar{\Lambda})^2 \frac{|\zeta^{(m)}(1)|^2}{4} - 6 \sum_p (\bar{\Lambda}'^{(p)} - \bar{\Lambda})^2 \frac{|\tau^{(p)}(1)|^2}{3} + \dots, \quad (5.9)$$

whereas  $m_c \gg m_b \gg \Lambda_{\text{QCD}}$  gives [2]

$$\lambda_1 + 3\lambda_2 = -9 \sum_m (\bar{\Lambda}^{*(m)} - \bar{\Lambda})^2 \frac{|\zeta^{(m)}(1)|^2}{4} + \dots. \quad (5.10)$$

These relations can be combined to obtain a sum rule for  $\lambda_2$ ,

$$\lambda_2 = -2 \sum_m (\bar{\Lambda}^{*(m)} - \bar{\Lambda})^2 \frac{|\zeta^{(m)}(1)|^2}{4} + 2 \sum_p (\bar{\Lambda}'^{(p)} - \bar{\Lambda})^2 \frac{|\tau^{(p)}(1)|^2}{3} + \dots. \quad (5.11)$$

Eqs. (5.9) and (5.11) were previously obtained in Ref. [32] using different methods. The strongest constraint on  $\lambda_1$  is given by Eq. (5.10) (the sum rule in Eq. (5.9) only implies  $-\lambda_1 > (0.06 + 0.15) \text{ GeV}^2$ ). Including the contribution of the lightest  $s_{\ell}^{\pi\ell} = \frac{1}{2}^+$  doublet to Eq. (5.10) yields

$$\lambda_1 < -3\lambda_2 - 9(\bar{\Lambda}^* - \bar{\Lambda})^2 \frac{|\zeta(1)|^2}{4} \simeq -3\lambda_2 - 0.18 \text{ GeV}^2, \quad (5.12)$$

neglecting perturbative QCD corrections. Note that only the broad  $D_1^*$  state (and its radial excitations) contribute to this sum rule, so the result in Eq (5.12) is sensitive to the relation between  $\tau(1)$  and  $\zeta(1)$  in Eq. (3.22).

Perturbative corrections to the sum rules in this section can be found in Ref. [33].

## VI. SUMMARY AND CONCLUSIONS

The branching ratios for  $B \rightarrow D e \bar{\nu}_e$  and  $B \rightarrow D^* e \bar{\nu}_e$  are  $(1.8 \pm 0.4)\%$  and  $(4.6 \pm 0.3)\%$ , respectively [9]. This implies that about 40% of semileptonic  $B$  decays are to excited charmed mesons and non-resonant final states. An excited charmed meson doublet ( $D_1(2420), D_2^*(2460)$ ) with  $s_{\ell}^{\pi\ell} = \frac{3}{2}^+$  has been observed. These states are narrow and have widths around 20 MeV. With some assumptions, the CLEO and ALEPH collaborations have measured about a  $(0.6 \pm 0.1)\%$  branching ratio for  $B \rightarrow D_1 e \bar{\nu}_e$ . The decay  $B \rightarrow D_2^* e \bar{\nu}_e$  has not been observed, and CLEO and ALEPH respectively report limits of 1% and 0.2% on



its branching ratio. A detailed experimental study of semileptonic  $B$  decays to these states should be possible in the future.

The semileptonic  $B$  decay rate to an excited charmed meson is determined by the corresponding matrix elements of the weak axial-vector and vector currents. At zero recoil (where the final excited charmed meson is at rest in the rest frame of the initial  $B$  meson), these currents correspond to charges of the heavy quark spin-flavor symmetry. Consequently, in the  $m_Q \rightarrow \infty$  limit, the zero recoil matrix elements of the weak currents between a  $B$  meson and any excited charmed meson vanish. However, at order  $\Lambda_{\text{QCD}}/m_Q$  these matrix elements are not necessarily zero. Since for  $B$  semileptonic decay to excited charmed mesons most of the available phase space is near zero recoil, the  $\Lambda_{\text{QCD}}/m_Q$  corrections can play a very important role. In this paper we studied the predictions of HQET for the  $B \rightarrow D_1 e \bar{\nu}_e$  and  $B \rightarrow D_2 e \bar{\nu}_e$  differential decay rates including the effects of  $\Lambda_{\text{QCD}}/m_Q$  corrections to the matrix elements of the weak currents. Since the matrix elements of the weak currents between a  $B$  meson and any excited charmed meson can only be nonzero for spin zero or spin one charmed mesons at zero recoil, the  $\Lambda_{\text{QCD}}/m_Q$  corrections are more important for the spin one member of the  $s_\ell^{\pi_\ell} = \frac{3}{2}^+$  doublet.

The  $\Lambda_{\text{QCD}}/m_Q$  corrections to the matrix elements of the weak axial-vector and vector currents can be divided into two classes; corrections to the currents themselves and corrections to the states. For  $B$  semileptonic decays to the  $D_1$ , parity invariance of the strong interactions forces the corrections to the states to vanish at zero recoil. Furthermore, the corrections to the current give a contribution which at zero recoil is expressible in terms of the leading,  $m_Q \rightarrow \infty$ , Isgur-Wise function and known meson mass splittings. This correction leads to an enhancement of the  $B$  semileptonic decay rate to the  $D_1$  over that to the  $D_2$ . With some model dependent assumptions, we made predictions for the differential decay rates for  $B \rightarrow D_1 e \bar{\nu}_e$  and  $B \rightarrow D_2^* e \bar{\nu}_e$  and determined the zero recoil value of the leading  $m_Q \rightarrow \infty$  Isgur-Wise function from the measured  $B$  to  $D_1$  semileptonic decay rate. The influence of perturbative QCD corrections on these decay rates were also considered but these are quite small.

Factorization was used to predict the rates for the nonleptonic decays  $B \rightarrow D_1 \pi$  and  $B \rightarrow D_2^* \pi$ . The ALEPH limit on the semileptonic decay rate to  $D_2^*$  implies a small branching ratio for  $B \rightarrow D_2^* \pi$ . The ratio  $\mathcal{B}(B \rightarrow D_1 \pi)/\mathcal{B}(B \rightarrow D_1 e \bar{\nu}_e)$  can be used to determine  $\hat{\tau}'$ . The present experimental value for this quantity favors  $\hat{\tau}'$  near  $-1.5$ .

The most significant uncertainty at order  $\Lambda_{\text{QCD}}/m_Q$  arises from  $\hat{\tau}_1$  and  $\hat{\eta}_{ke}$ . It may be possible to determine these quantities from measurements of  $R = \Gamma_{D_2^*}/\Gamma_{D_1}$  and  $\mathcal{B}(B \rightarrow D_2^* \pi)/\mathcal{B}(B \rightarrow D_1 \pi)$ . The  $w$ -dependence of the semileptonic decay rates can provide important similar information.

A broad multiplet of excited charmed mesons with masses near those of the  $D_1$  and  $D_2^*$  is expected. It has spin of the light degrees of freedom  $s_\ell^{\pi_\ell} = \frac{1}{2}^+$ , giving spin zero and spin one states that are usually denoted by  $D_0^*$  and  $D_1^*$ . We studied the predictions of HQET for the  $B \rightarrow D_0^* e \bar{\nu}_e$  and  $B \rightarrow D_1^* e \bar{\nu}_e$  differential decay rates including the effects of  $\Lambda_{\text{QCD}}/m_Q$  corrections to the matrix elements of the weak current. The situation here is similar to that in the case of the  $s_\ell^{\pi_\ell} = \frac{3}{2}^+$  doublet. Using a relation between the leading,  $m_Q \rightarrow \infty$ , Isgur-Wise functions for these two excited charmed meson doublets that is valid in the nonrelativistic constituent quark model with any spin-orbit independent potential (and a

Approximation	$R = \Gamma_{D_2^*}/\Gamma_{D_1}$	$\tau(1) \left[ \frac{6.0 \times 10^{-3}}{\mathcal{B}(B \rightarrow D_1 e \bar{\nu}_e)} \right]^{1/2}$	$\Gamma_{D_1+D_2^*+D_1^*+D_0^*}/\Gamma_{D_1}$
$B_\infty$	1.65	1.24	4.26
$B_1$	0.52	0.71	2.55
$B_2$	0.67	0.75	2.71

TABLE VI. Predictions for  $\Gamma_{D_2^*}/\Gamma_{D_1}$ ,  $\tau(1)$ , and  $\Gamma_{D_1+D_2^*+D_1^*+D_0^*}/\Gamma_{D_1}$  using  $\hat{\tau}' = -1.5$ . The results in the last column assume the nonrelativistic quark model prediction in Eq. (3.22).

few other assumptions), we determined the rates for  $B$  semileptonic decays to these excited charmed mesons. We find that branching ratio for  $B$  semileptonic decays into the four states in the  $s_\ell^{\pi_\ell} = \frac{1}{2}^+$  and  $\frac{3}{2}^+$  doublets is about 1.6%. Combining this with the measured rates to the ground state  $D$  and  $D^*$  implies that more than 2% of the  $B$  meson decays must be semileptonic decays to higher mass excited charmed states or nonresonant modes. Some of the more important results in Tables II and IV are summarized in Table VI.

We considered the zero recoil matrix elements of the weak currents between a  $B$  meson and other excited charmed mesons at order  $\Lambda_{\text{QCD}}/m_Q$ . Only the corrections to the states contribute and these were expressed in terms of matrix elements of local operators.

Our results have implications for  $B$  decay sum rules, where including the contributions of the excited charmed meson states strengthens the bounds on  $\rho^2$  (the slope of the Isgur-Wise function for  $B \rightarrow D^{(*)} e \bar{\nu}_e$ ), on  $\lambda_1$ , and on the zero recoil matrix element of the axial-vector current between  $B$  and  $D^*$  mesons. The latter bound has implications for the extraction of  $|V_{cb}|$  from exclusive  $B \rightarrow D^* e \bar{\nu}_e$  decay.

## ACKNOWLEDGMENTS

We thank A. Le Yaouanc, M. Neubert, A. Vainshtein for useful discussions, and A. Falk for keeping us from being disingenuous. This work was supported in part by the Department of Energy under grant no. DE-FG03-92-ER 40701.

## APPENDIX A: PERTURBATIVE ORDER $\alpha_s$ CORRECTIONS

In this Appendix we compute order  $\alpha_s$  and order  $\alpha_s \Lambda_{\text{QCD}}/m_Q$  corrections to the  $B \rightarrow (D_1, D_2^*) e \bar{\nu}_e$  form factors. At this order both the current in Eq. (2.7) and the order  $\Lambda_{\text{QCD}}/m_Q$  corrections to the Lagrangian in Eq. (1.4) receive corrections. Matrix elements of the kinetic energy operator,  $\eta_{\text{ke}}^{(Q)}$ , enter proportional to  $\tau$  to all orders in  $\alpha_s$  due to reparameterization invariance [34]. The matrix elements involving the chromomagnetic operator are probably very small and have been neglected. Order  $\alpha_s$  corrections to the  $b \rightarrow c$  flavor changing current in the effective theory introduce a set of new operators at each order in  $\Lambda_{\text{QCD}}/m_Q$ , with the appropriate dimensions and quantum numbers. The Wilson coefficients for these operators are known  $w$ -dependent functions [17,35], which we take from [36].

The vector and axial-vector currents can be written at order  $\alpha_s$  as

$$\begin{aligned}
V^\mu &= \bar{h}_{v'}^{(c)} \left[ \gamma^\mu - \frac{i \overleftarrow{\mathcal{D}} \gamma^\mu}{2 m_c} + \frac{i \gamma^\mu \overrightarrow{\mathcal{D}}}{2 m_b} \right] h_v^{(b)} + \frac{\alpha_s}{\pi} [V^{\mu(1)} + V^{\mu(2)}] + \dots, \\
A^\mu &= \bar{h}_{v'}^{(c)} \left[ \gamma^\mu \gamma_5 - \frac{i \overleftarrow{\mathcal{D}} \gamma^\mu \gamma_5}{2 m_c} + \frac{i \gamma^\mu \gamma_5 \overrightarrow{\mathcal{D}}}{2 m_b} \right] h_v^{(b)} + \frac{\alpha_s}{\pi} [A^{\mu(1)} + A^{\mu(2)}] + \dots, \tag{A1}
\end{aligned}$$

where the ellipses denote terms higher order in  $\alpha_s$  and  $\Lambda_{\text{QCD}}/m_Q$ . Superscripts (1) denote corrections proportional to  $\alpha_s$ ,

$$\begin{aligned}
V^{\mu(1)} &= \bar{h}_{v'}^{(c)} [c_{V1} \gamma^\mu + c_{V2} v^\mu + c_{V3} v'^\mu] h_v^{(b)}, \\
A^{\mu(1)} &= \bar{h}_{v'}^{(c)} [c_{A1} \gamma^\mu + c_{A2} v^\mu + c_{A3} v'^\mu] \gamma_5 h_v^{(b)}. \tag{A2}
\end{aligned}$$

The terms with superscript (2) in Eq. (A1) denote corrections proportional to  $\alpha_s \Lambda_{\text{QCD}}/m_Q$ ,

$$\begin{aligned}
V^{\mu(2)} &= \bar{h}_{v'}^{(c)} \left\{ \frac{i \overrightarrow{\mathcal{D}}_\lambda}{2 m_b} \left[ (c_{V1} \gamma^\mu + c_{V2} v^\mu + c_{V3} v'^\mu) \left( \gamma^\lambda + 2v'^\lambda \frac{\overleftarrow{\partial}}{\partial w} \right) + 2c_{V2} g^{\mu\lambda} \right] \right. \\
&\quad \left. - \frac{i \overleftarrow{\mathcal{D}}_\lambda}{2 m_c} \left[ 2c_{V3} g^{\mu\lambda} + \left( \gamma^\lambda + 2v^\lambda \frac{\overrightarrow{\partial}}{\partial w} \right) (c_{V1} \gamma^\mu + c_{V2} v^\mu + c_{V3} v'^\mu) \right] \right\} h_v^{(b)}, \tag{A3} \\
A^{\mu(2)} &= \bar{h}_{v'}^{(c)} \left\{ \frac{i \overrightarrow{\mathcal{D}}_\lambda}{2 m_b} \left[ (c_{A1} \gamma^\mu + c_{A2} v^\mu + c_{A3} v'^\mu) \gamma_5 \left( \gamma^\lambda + 2v'^\lambda \frac{\overleftarrow{\partial}}{\partial w} \right) + 2c_{A2} g^{\mu\lambda} \gamma_5 \right] \right. \\
&\quad \left. - \frac{i \overleftarrow{\mathcal{D}}_\lambda}{2 m_c} \left[ 2c_{A3} g^{\mu\lambda} + \left( \gamma^\lambda + 2v^\lambda \frac{\overrightarrow{\partial}}{\partial w} \right) (c_{A1} \gamma^\mu + c_{A2} v^\mu + c_{A3} v'^\mu) \right] \gamma_5 \right\} h_v^{(b)}.
\end{aligned}$$

In these expressions the covariant derivatives,  $D_\lambda$ , act on the fields  $h_v^{(b)}$  or  $h_{v'}^{(c)}$ , and partial derivatives with respect to  $w$ ,  $\partial/\partial w$ , act on the coefficient functions  $c_{Vi}(w)$  and  $c_{Ai}(w)$ . Using Eqs. (A2) and (A3) it is straightforward to include the order  $\alpha_s$  and  $\alpha_s \Lambda_{\text{QCD}}/m_Q$  corrections using trace formalism presented in Sec. II. The corrections with superscript (1) simply change the form of  $\Gamma$  in Eq. (2.6), while those with superscript (2) change  $\Gamma$  in Eq. (2.8).

The  $B \rightarrow D_1 e \bar{\nu}_e$  form factors were defined in Eq. (2.1), and their expansions in terms of Isgur-Wise functions at leading order in  $\alpha_s$  were given in Eq. (2.20). The order  $\alpha_s$  and order  $\alpha_s \Lambda_{\text{QCD}}/m_Q$  corrections modify the results for  $f_i$  in Eq. (2.20) to  $f_i + (\alpha_s/\pi) \delta f_i$ . The functions  $\delta f_i$  are given by

$$\begin{aligned}
\sqrt{6} \delta f_A &= -(w+1)c_{A1}\tau - 2\varepsilon_c(w\bar{\Lambda}' - \bar{\Lambda})[2c_{A1} + (w+1)c'_{A1} + c_{A3}]\tau \\
&\quad + \varepsilon_c(w-1)\{[3c_{A1} - 2(w-1)c_{A3}]\tau_1 - (3c_{A1} + 4c_{A3})\tau_2\} \\
&\quad - \varepsilon_b[(\bar{\Lambda}' + \bar{\Lambda})(w-1)c_{A1} - 2(\bar{\Lambda}' - w\bar{\Lambda})(w+1)c'_{A1} + 2(w\bar{\Lambda}' - \bar{\Lambda})c_{A2}]\tau \\
&\quad + \varepsilon_b(w-1)\{[(2w+1)c_{A1} - 2(w-1)c_{A2}]\tau_1 + (c_{A1} - 4c_{A2})\tau_2\}, \tag{A4}
\end{aligned}$$

$$\begin{aligned}
\sqrt{6} \delta f_{V_1} &= (1-w^2)c_{V1}\tau - 2\varepsilon_c(w\bar{\Lambda}' - \bar{\Lambda})(w+1)[2c_{V1} + (w-1)c'_{V1} + 2c_{V3}]\tau \\
&\quad + \varepsilon_c(w^2-1)\{[3c_{V1} + 2(w+2)c_{V3}]\tau_1 - (3c_{V1} + 2c_{V3})\tau_2\} \\
&\quad - \varepsilon_b(w+1)[(\bar{\Lambda}' + \bar{\Lambda})(w-1)c_{V1} - 2(\bar{\Lambda}' - w\bar{\Lambda})(w-1)c'_{V1} + 4(w\bar{\Lambda}' - \bar{\Lambda})c_{V2}]\tau \\
&\quad + \varepsilon_b(w^2-1)\{[(2w+1)c_{V1} + 2(w+2)c_{V2}]\tau_1 + (c_{V1} - 2c_{V2})\tau_2\}, \tag{A5}
\end{aligned}$$

$$\begin{aligned}
\sqrt{6} \delta f_{V_2} = & -[3c_{V_1} + 2(w+1)c_{V_2}]\tau - 2\varepsilon_c (w\bar{\Lambda}' - \bar{\Lambda}) [3c'_{V_1} + 2c_{V_2} + 2(w+1)c'_{V_2}]\tau \\
& - \varepsilon_c \left\{ [(4w-1)c_{V_1} - 2(2w+1)(w-1)c_{V_2} - 2(w+2)c_{V_3}]\tau_1 \right. \\
& \quad \left. + [5c_{V_1} + 2(1-w)c_{V_2} + 2c_{V_3}]\tau_2 \right\} \\
& - \varepsilon_b \left\{ 3(\bar{\Lambda}' + \bar{\Lambda})c_{V_1} - 6(\bar{\Lambda}' - w\bar{\Lambda})c'_{V_1} + 2[(w-1)\bar{\Lambda}' + (3w+1)\bar{\Lambda}]c_{V_2} \right. \\
& \quad \left. - 4(\bar{\Lambda}' - w\bar{\Lambda})(w+1)c'_{V_2} \right\} \tau \\
& + \varepsilon_b \left\{ [3(2w+1)c_{V_1} + 2(2w^2+1)c_{V_2}]\tau_1 + [3c_{V_1} + 2(w-2)c_{V_2}]\tau_2 \right\}, \tag{A6}
\end{aligned}$$

$$\begin{aligned}
\sqrt{6} \delta f_{V_3} = & [(w-2)c_{V_1} - 2(w+1)c_{V_3}]\tau \\
& + 2\varepsilon_c (w\bar{\Lambda}' - \bar{\Lambda}) \left\{ 2c_{V_1} + (w-2)c'_{V_1} - 2[c_{V_3} + (w+1)c'_{V_3}] \right\} \tau \\
& + \varepsilon_c \left\{ [(2+w)c_{V_1} + 2(w^2-3w-1)c_{V_3}]\tau_1 + [(3w+2)c_{V_1} + (4w-2)c_{V_3}]\tau_2 \right\} \\
& + \varepsilon_b \left[ (\bar{\Lambda}' + \bar{\Lambda})(w+2)c_{V_1} + 2(\bar{\Lambda}' - w\bar{\Lambda})(2-w)c'_{V_1} + 4\bar{\Lambda}'(w+1)c_{V_2} \right. \\
& \quad \left. - 2(\bar{\Lambda}' + \bar{\Lambda})(w-1)c_{V_3} + 4(\bar{\Lambda}' - w\bar{\Lambda})(w+1)c'_{V_3} \right] \tau \\
& - \varepsilon_b \left\{ [(2w^2+5w+2)c_{V_1} + 2w(2+w)c_{V_2} + 2(1+w-2w^2)c_{V_3}]\tau_1 \right. \\
& \quad \left. + [(2+w)c_{V_1} - 2wc_{V_2} - 2(w-1)c_{V_3}]\tau_2 \right\}. \tag{A7}
\end{aligned}$$

Here  $c_{V_i}$  and  $c_{A_i}$  are functions of  $w$ , and prime denotes a derivative with respect to  $w$ . Note that at zero recoil  $\delta f_{V_i}$  is known in terms of  $\bar{\Lambda}' - \bar{\Lambda}$  and  $\tau(1)$ , as expected from our results in Sec. II.

For  $B \rightarrow D_2^* e \bar{\nu}_e$  decay, the  $\alpha_s$  and order  $\alpha_s \Lambda_{\text{QCD}}/m_Q$  corrections modify the leading order form factors in Eq. (2.21) to  $k_i \rightarrow k_i + (\alpha_s/\pi) \delta k_i$ . The functions  $\delta k_i$  are

$$\begin{aligned}
\delta k_V = & -c_{V_1}\tau - \varepsilon_c \left[ 2c'_{V_1}(w\bar{\Lambda}' - \bar{\Lambda})\tau + (c_{V_1} - 2wc_{V_3})\tau_1 - (c_{V_1} + 2c_{V_3})\tau_2 \right] \\
& - \varepsilon_b \left\{ [(\bar{\Lambda}' + \bar{\Lambda})c_{V_1} - 2(\bar{\Lambda}' - w\bar{\Lambda})c'_{V_1}]\tau - [(2w+1)c_{V_1} + 2wc_{V_2}]\tau_1 - (c_{V_1} + 2c_{V_2})\tau_2 \right\}, \tag{A8}
\end{aligned}$$

$$\begin{aligned}
\delta k_{A_1} = & -(w+1)c_{A_1}\tau - \varepsilon_c \left[ 2(c'_{A_1} + wc'_{A_1} - c_{A_3})(w\bar{\Lambda}' - \bar{\Lambda})\tau + (w-1)c_{A_1}(\tau_1 - \tau_2) \right. \\
& \quad \left. + 2(w^2-1)c_{A_3}\tau_1 \right] - \varepsilon_b \left\{ [(\bar{\Lambda}' + \bar{\Lambda})(w-1)c_{A_1} - 2(\bar{\Lambda}' - w\bar{\Lambda})(w+1)c'_{A_1} \right. \\
& \quad \left. - 2(w\bar{\Lambda}' - \bar{\Lambda})c_{A_2}]\tau - (w-1)[c_{A_1}(\tau_1 + \tau_2) + 2(wc_{A_1} - wc_{A_2} - c_{A_2})\tau_1] \right\}, \tag{A9}
\end{aligned}$$

$$\begin{aligned}
\delta k_{A_2} = & c_{A_2}\tau + \varepsilon_c \left\{ 2c'_{A_2}(w\bar{\Lambda}' - \bar{\Lambda})\tau - [2c_{A_1} - (2w+1)c_{A_2} + 2c_{A_3}]\tau_1 + c_{A_2}\tau_2 \right\} \\
& + \varepsilon_b \left\{ [(\bar{\Lambda}' + 3\bar{\Lambda})c_{A_2} - 2(\bar{\Lambda}' - w\bar{\Lambda})c'_{A_2}]\tau - (2w+3)c_{A_2}\tau_1 - c_{A_2}\tau_2 \right\}, \tag{A10}
\end{aligned}$$

$$\begin{aligned}
\delta k_{A_3} = & (c_{A_1} + c_{A_3})\tau + \varepsilon_c \left[ 2(c'_{A_1} + c'_{A_3})(w\bar{\Lambda}' - \bar{\Lambda})\tau - (c_{A_1} - c_{A_3})(\tau_1 + \tau_2) + 4wc_{A_3}\tau_1 \right] \\
& + \varepsilon_b \left\{ [(\bar{\Lambda}' + \bar{\Lambda})(c_{A_1} + c_{A_3}) - 2\bar{\Lambda}'c_{A_2} - 2(\bar{\Lambda}' - w\bar{\Lambda})(c'_{A_1} + c'_{A_3})]\tau \right. \\
& \quad \left. - (c_{A_1} + c_{A_3})(\tau_1 + \tau_2) - 2w(c_{A_1} - c_{A_2} + c_{A_3})\tau_1 \right\}. \tag{A11}
\end{aligned}$$

To compute the corrections to the results obtained in Sec. II, it is sufficient to expand the Wilson coefficients  $c_{V_i}$  and  $c_{A_i}$  to linear order in  $w$ . We take  $c_{V_i}$  and  $c_{A_i}$  and their first derivatives at zero recoil from Ref. [36]. To evaluate these, we choose to integrate out the  $c$  and  $b$  quarks at a common scale  $\mu = \sqrt{m_c m_b}$ , giving for  $c_{V_i}$  and  $c_{A_i}$

$$\begin{aligned}
c_{V1}(1) &= -\frac{4}{3} - \frac{1+z}{1-z} \ln z \simeq 0.91, \\
c_{V2}(1) &= -\frac{2(1-z+z \ln z)}{3(1-z)^2} \simeq -0.46, \\
c_{V3}(1) &= \frac{2z(1-z+\ln z)}{3(1-z)^2} \simeq -0.20, \\
c_{A1}(1) &= -\frac{8}{3} - \frac{1+z}{1-z} \ln z \simeq -0.42, \\
c_{A2}(1) &= -\frac{2[3-2z-z^2+(5-z)z \ln z]}{3(1-z)^3} \simeq -1.20, \\
c_{A3}(1) &= \frac{2z[1+2z-3z^2+(5z-1) \ln z]}{3(1-z)^3} \simeq 0.42.
\end{aligned} \tag{A12}$$

The derivatives  $c'_{V_i}$  and  $c'_{A_i}$  at zero recoil are

$$\begin{aligned}
c'_{V1}(1) &= -\frac{2[13-9z+9z^2-13z^3+3(2+3z+3z^2+2z^3) \ln z]}{27(1-z)^3} \simeq 0.20, \\
c'_{V2}(1) &= \frac{2[2+3z-6z^2+z^3+6z \ln z]}{9(1-z)^4} \simeq 0.21, \\
c'_{V3}(1) &= \frac{2z[1-6z+3z^2+2z^3-6z^2 \ln z]}{9(1-z)^4} \simeq 0.05, \\
c'_{A1}(1) &= -\frac{2[7+9z-9z^2-7z^3+3(2+3z+3z^2+2z^3) \ln z]}{27(1-z)^3} \simeq 0.64, \\
c'_{A2}(1) &= \frac{2[2-33z+9z^2+25z^3-3z^4-6z(1+7z) \ln z]}{9(1-z)^5} \simeq 0.37, \\
c'_{A3}(1) &= -\frac{2z[3-25z-9z^2+33z^3-2z^4-6z^2(7+z) \ln z]}{9(1-z)^5} \simeq -0.12.
\end{aligned} \tag{A13}$$

Here  $z = m_c/m_b$ , and the numbers quoted are for  $z = 1.4/4.8$ .

Using these values and the  $\alpha_s$  corrections for the form factors above, we find the corrections given in Table III to the leading order results summarized in Table II.

## REFERENCES

- [1] N. Isgur and M.B. Wise, Phys. Lett. B232 (1989) 113; Phys. Lett. B237 (1990) 527.
- [2] A.K. Leibovich *et al.*, Phys. Rev. Lett. 78 (1997) 3995.
- [3] N. Isgur and M.B. Wise, Phys. Rev. Lett. 66 (1991) 1130.
- [4] E. Eichten and B. Hill, Phys. Lett. B234 (1990) 511;  
H. Georgi, Phys. Lett. B240 (1990) 447.
- [5] E. Eichten and B. Hill, Phys. Lett. B243 (1990) 427;  
A.F. Falk *et al.*, Nucl. Phys. B357 (1991) 185.
- [6] M. Feindt, Talk given at the Second International Conference on *B* physics and *CP* violation, Honolulu, March 1997;  
G. Eigen, Talk given at the Seventh International Symposium on Heavy Flavor Physics, Santa Barbara, July 1997.
- [7] M. Gremm *et al.*, Phys. Rev. Lett. 77 (1996) 20;  
M. Gremm and I. Stewart, Phys. Rev. D55 (1997) 1226.
- [8] M. Gremm and A. Kapustin, Phys. Rev. D55 (1997) 6924.
- [9] Particle Data Group, R.M. Barnett *et al.*, Phys. Rev. D54 (1996) 1.
- [10] S. Nussinov and W. Wetzel, Phys. Rev. D36 (1987) 130.
- [11] M. Voloshin and M. Shifman, Sov. J. Nucl. Phys. 47 (1988) 511.
- [12] M.E. Luke, Phys. Lett. B252 (1990) 447.
- [13] CLEO Collaboration, J.E. Duboscq *et al.*, Phys. Rev. Lett. 76 (1996) 3898;  
J.D. Richman, and P.R. Burchat, Rev. Mod. Phys. 67 (1995) 893.
- [14] OPAL Collaboration, R. Akers *et al.*, Z. Phys. C67 (1995) 57.
- [15] ALEPH Collaboration, D. Buskulic *et al.*, Z. Phys. C73 (1997) 601.
- [16] CLEO Collaboration, T.E. Browder *et al.*, Report no. CLEO CONF 96-2, ICHEP96 PA05-077.
- [17] A.F. Falk *et al.*, Nucl. Phys. B343 (1990) 1.
- [18] J.D. Bjorken, *Proceedings of the 18th SLAC Summer Institute on Particle Physics*, pp. 167, Stanford, July 1990, ed. by J.F. Hawthorne (SLAC, Stanford, 1991);  
A.F. Falk, Nucl. Phys. B378 (1992) 79.
- [19] N. Isgur and M.B. Wise, Phys. Rev. D43 (1991) 819.
- [20] T. Mannel and W. Roberts, Z. Phys. C61 (1994) 293.
- [21] M. Neubert *et al.*, Phys. Lett. B301 (1993) 101; Phys. Rev. D47 (1993) 5060.
- [22] N. Isgur *et al.*, Phys. Rev. D39 (1989) 799;  
D. Scora and N. Isgur, Phys. Rev. D52 (1995) 2783.
- [23] P. Colangelo *et al.*, Phys. Lett. B293 (1992) 207.
- [24] S. Veseli and M.G. Olsson, Phys. Lett. B367 (1996) 302; Phys. Rev. D54 (1996) 886.
- [25] V. Morenas *et al.*, Phys. Lett. B386 (1996) 315; hep-ph/9706265.
- [26] S. Godfrey and N. Isgur, Phys. Rev. D32 (1985) 189;  
S. Godfrey and Kokoski, Phys. Rev. D43 (1991) 1679;  
A.B. Kaidalov and A.V. Nogteva, Sov. J. Nucl. Phys. 47 (1988) 321;  
J. Rosner, Comments Nucl. Part. Phys. 16 (1986) 109.
- [27] M.J. Dugan and B. Grinstein, Phys. Lett. B255 (1991) 583.
- [28] CLEO Collaboration, J. Gronberg *et al.*, Report no. CLEO CONF 96-25, ICHEP96 PA05-069.

- [29] J.D. Bjorken, Invited talk at Les Rencontre de la Valle d'Aoste (La Thuile, Italy), SLAC-PUB-5278 (1990).
- [30] M.B. Voloshin, Phys. Rev. D46 (1992) 3062.
- [31] I.I. Bigi *et al.*, Phys. Rev. D52 (1995) 196.
- [32] I. Bigi *et al.*, TPI-MINN-97-02-T [hep-ph/9703290].
- [33] A. Kapustin *et al.*, Phys. Lett. B375 (1996) 327;  
C.G. Boyd *et al.*, Phys. Rev. D55 (1997) 3027;  
A. Czarnecki *et al.*, TPI-MINN-97-19 [hep-ph/9706311].
- [34] M. Luke and A.V. Manohar, Phys. Lett. B286 (1992) 348.
- [35] A.F. Falk and B. Grinstein, Phys. Lett. B247 (1990) 406;  
M. Neubert, Phys. Lett. B306 (1993) 357; Nucl. Phys. B416 (1994) 786.
- [36] M. Neubert, Phys. Rept. 245 (1994) 259; and references therein.